PONTIFICIA UNIVERSIDAD CATOLICA DE CHILE
Facultad de Ciencias Biológicas
Programa Doctorado en Ciencias Biológicas
Departamento Genética Molecular y Microbiología

Nitrate-mediated shoot growth is modulated by cell expansion and endoreplication in *Arabidopsis thaliana*.

Tesis entregada a la Pontificia Universidad Católica de Chile en cumplimiento parcial de los requisitos para optar al Grado de Doctor en Ciencias con mención en Genética Molecular y Microbiología

By:

Sebastián Andrés Moreno Ramírez

…Los animales se dividen en
(a) pertenecientes al Emperador,
(b) embalsamados, (c) amaestrados, (d) lechones, (e) sirenas,
(f) fabulosos, (g) perros sueltos,
(h) incluidos en esta clasificación, (i) que se agitan como locos,
(j) innumerables,
(k) dibujados con un pincel finísimo de pelo de camello,
(l) etcétera, (m) que acaban de romper el jarrón,
(n) que de lejos parecen moscas…

AGRADECIMIENTOS

Quisiera tomarte estas breves líneas para agradecer a los que hicieron de esta tesis un proceso ameno y entretenido. A todas las personas que me han alentado a seguir el camino de la ciencia, a seguir aprendiendo, a mantener la curiosidad. A todos ellos éstas breves palabras.

En primer lugar, a mis padres, por siempre estar alentándome a seguir mis sueños, por animarme cuando la tesis se veía cuesta arriba y por simplemente estar ahí, por ser. Los amo.

A mis hermanos, por ser la mejor pandilla de diversidad que uno podría querer, por hacer de la discusión una mufa constante y de la diferencia un aliado fiel.

A mi familia en general, por simplemente preguntar cómo uno va, por los asados domingueros y no tan domingueros. Que el tango y los boleros se escuchen fuerte. Lito querido.

A mis amigos que me hicieron olvidar la tesis cuando era necesario, que me sacaron risas y llantos de alegría. A mis amigos científicos que hicieron todo lo contrario, desde cuestionarme experimentos hasta nuevas teorías. En especial a esos filósofos de la ciencia, esos que permitieron el continuo encanto del pensar, el constante cuestionamiento de la técnica y la incansable torcedura de lo supuesto.

A mis compañeros y amigos de laboratorio, por hacer la vida en el laboratorio un carrusel de emociones, por hacer del laboratorio el mejor gimnasio, el mejor bar, el mejor “after”, la mejor pizzería. Que siga el ánimo, mil gracias.

A mi tutor Rodrigo, por confiar en mi. Gracias por todas esas críticas, consejos y discusiones científicas, tanto por las que llegaron a puerto, como por las que no.

Por último, a Carla, mi compañera, por estar siempre ahí, por dejarme ser parte de tu vida. Con la tesis no solo comencé una historia científica, comencé también una historia contigo. Ha seguiremos disfrutándola.

Gracias totales.

INDEX

RESUMEN

Cómo los organismos saben cuándo sus tejidos han alcanzado su tamaño final es una pregunta fundamental y aún sin resolver en biología del desarrollo. En organismos multicelulares, señales ambientales e internas son integradas para modular el crecimiento de órganos y tejidos. Está muy bien reportado que el ambiente nutricional en el que crecen los organismos modula el crecimiento y tamaño de los órganos. En plantas, sin embargo, los mecanismos moleculares que explican la interconectividad y coordinación entre señales ambientales y crecimiento siguen sin ser comprendidas. Nitrato es una fuente nutricional clave limitante del crecimiento y productividad de las plantas tanto en ambientes naturales como en sistemas agrícolas. Además de su rol como nutriente, nitrato puede actuar como una señal molecular que desencadena cambios a nivel de expresión génica, metabolismo, fisiológicos y de desarrollo. Aunque muchos procesos son modulados por nitrato, una conectividad entre la dinámica celular, el tamaño de los órganos y el nitrato nunca ha sido reportada.

En el presente trabajo nos centramos en el tejido vegetativo como modelo de estudio de los procesos de desarrollo modulados por la disponibilidad del nitrato. Para entender cómo nitrato regula el tejido vegetativo, se realizó un experimento en el cual se crecieron plantas en distintas concentraciones de nitrato y se cuantificó el área del tejido aéreo desde 3 a 7 días post-imbibición. Curiosamente, observamos que el área del tejido vegetativo empieza a divergir entre las 3 condiciones nutricionales al día 5 aproximadamente. Al final del curso temporal observamos que las plantas son totalmente distintas con una respuesta dependiente de la concentración de nitrato.

Para entender cómo nitrato aumenta el tamaño del tejido vegetativo durante el curso temporal previamente mencionado, se realizó un análisis de “ cotyledon live-imaging” a través de microscopía confocal en las células epidermales del tejido vegetativo. Por medio de líneas

reporteras transgénicas logramos seguir la dinámica celular y nuclear del mismo grupo de células a través del curso temporal de cinco días en condiciones contrastantes de nitrato (0 y 5 mM). El análisis de "live-imaging" nos permitió determinar que el crecimiento del tejido vegetativo observado se debe exclusivamente a una expansión celular, descartando la división celular como un proceso relevante durante el crecimiento mediado por nitrato durante esta etapa del desarrollo. En plantas, se ha correlacionado la expansión celular con el proceso de endoreplicación, el que consiste en un ciclo celular modificado en el cual las células pasan por continuas rondas de replicación de su material genético, sin pasar por la etapa mitótica. A través de análisis de citometría de flujo, determinamos que efectivamente un aumento del nitrato incrementa los niveles de ploidía, explicando el aumento en el tamaño celular observado previamente.

Posteriormente, para identificar el mecanismo por el cual nitrato aumenta los niveles de ploidía y área celular, se realizó un análisis transcripcional por RNA-seq en plantas con y sin nitrato al inicio del curso temporal. Al analizar si la expresión de genes del ciclo celular estaba siendo modificada por la presencia de nitrato, encontramos que el gen *LGO* (Loss of Giant cells from Organs) estaba diferencialmente expresado en respuesta a nitrato. Se ha reportado previamente que LGO es gen esencial para el proceso de expansión celular y endoreplicación en sépalos. LGO, sin embargo, no ha sido asociado a nitrato ni a la etapa de desarrollo en la que se ha realizado el presente trabajo. Análisis de citometría de flujo en las mutantes *lgo-2* confirmaron que LGO es un gen esencial para los procesos de expansión celular y endoreplicación en respuesta a nitrato.

Curiosamente, a pesar de que la mutante *lgo-2* tiene menores niveles de ploidía y células considerablemente más pequeñas que en plantas silvestre, el tamaño del tejido vegetativo es igual entre ambos genotipos acorde a las concentraciones de nitrato. Con el fin de entender mejor la dinámica celular que ocurre en la mutante *lgo-2* se realizó la misma aproximación de "live-

imaging" pero ahora utilizando la mutante *lgo-2* transformada con los reporteros para el seguimiento de la dinámica celular y nuclear. Observamos que en la mutante *lgo-2* ocurre una compensación a través de proliferación celular para alcanzar el tamaño del tejido vegetativo acorde a la concentración de nitrato. En consecuencia, el tejido vegetativo alcanza un tamaño dependiendo del nitrato disponible, ya sea por expansión celular o por división celular como se observó en plantas silvestres y mutante respectivamente.

El presente trabajo proporciona un punto de entrada hacia el mejor entendimiento del rol de nitrato en el control del tamaño del tejido aéreo, relación que no ha sido explorada hasta el momento. Entender como el tejido vegetativo responde a la disponibilidad nutricional de nitrato es de vital importancia para la producción agrícola y futuras aplicaciones biotecnológicas.

ABSTRACT

How organisms know when they have reached right organ size is a key question in developmental biology. In multicellular organism, environmental and internal cues are integrated to modulate organ growth. It has been extensively reported that nutritional status regulates organ growth and development. In plants, the molecular mechanism underlying connectivity and coordination between nutrient signaling and organ size is still unknown. Nitrogen is the main macronutrient for plant growth and basic metabolic processes. Nitrate (NO_3^-) is the main source of nitrogen for plants in many natural environmental as well as agricultural systems. Besides its role as a nutrient, nitrate treatments trigger local and systemic signaling pathways that modulate gene expression, metabolism, physiology as well as growth and developmental processes in plants. Despite many developmental processes have been associated to nitrate, the interplay between cellular dynamic, shoot growth and nitrate has never been assessed.

We have focused this study on the understanding of how nitrate modulates shoot growth. In order to understand how nitrate regulates vegetative tissue, we conducted an experiment in which we grew plants under contrasting concentrations of nitrate. Shoot area was quantified in the different nitrate conditions from 3 to 7 days after sowing (DAS). Interestingly, shoot area was similar for all nitrate conditions 3 DAS. Around day 5 shoot size started to increase in a nitrate-dependent manner.

In order to understand the mechanism underlying shoot growth triggered by nitrate, we performed a cotyledon live-imaging approach through confocal microscopy. We imaged the same spot of epidermal cells during the temporal-course mentioned above from plants grown under 0 and 5 mM nitrate. Through double reporter lines for plasma membrane and nuclei, we were able

to track cellular and nuclei dynamics for the same spot of epidermal cells. The cotyledon live-imaging approach allowed us to determine that nitrate-mediated shoot growth is elicited exclusively by cell expansion. We discarded cell division as a relevant process during the assessed developmental stage.

In plants, cell expansion is often associated to a process called endoreplication, which consist in a modified cell cycle, cells going through continues round of DNA replication and skipping mitotic stage. Using flow cytometry technology, we showed that nitrate promotes endoreplication in shoot cells. We observed that plants grown in the presence of nitrate have higher-order ploidy levels than plants grown in the absence of this nutrient. Then, to gain insight into the mechanism behind nitrate-elicited regulation of ploidy and cell expansion, we conducted a RNA-seq approach to see whether cell cycle genes related to endoreplication and cell expansion were regulated by nitrate. We observed that the gene *LOSS OF GIANT CELLS FROMS ORGANS* (*LGO*) was regulated in response to nitrate. LGO has been previously associated to endoreplication and cell expansion during sepal development. However, this cell cycle gene has never been related to nitrate or post-embryonic developmental stages. Flow cytometry analysis of *lgo-2* mutant plants confirmed that LGO is essential for nitrate-mediated cell expansion and endoreplication.

Despite endoreplication and cell expansion processes are strongly disrupted in *lgo-2* mutant plants, shoot size is similar in *lgo-2* and to wild-type plants for all nitrate concentrations. In order to understand the cellular dynamic behind the compensation process observed in *lgo-2* mutant plants, we performed a new cotyledon live-imaging approach with the same double reporter mentioned above in *lgo-2* plants as background. In the absence of LGO, organ size is reached through increased cell division in pavement cells. Thus, organ size is defined by nutritional status

and it can be reached either by cell expansion or cell division, as we observed for wild-type or *lgo-2 plants* respectively.

Our results provide an entry point towards better understanding of the role of nitrate in controlling shoot size, which has not been explored thus far. Understanding above-ground plant size in response to N-availability is important for crop yield. Our work represents a first step towards developing biotechnological solutions to improve nitrogen use efficiency for sustainable agriculture.

INTRODUCTION

Internal and environmental signals are sensed and integrated to modulate organ growth and size. In plants, these different signals are thought to modulate organ growth through adjusting cell proliferation and cell expansion (Czesnick and Lenhard, 2015). Knowledge is still limited regarding how environmental cues modulate organ size. For instance, nutrient modulation of organ growth and size has been extensively documented, yet little progress has been made towards comprehension of the molecular mechanism underlying organ growth and size in response to nutrient availability.

The mineral nutrient required in the greatest abundance by plants is nitrogen (N) (Epstein and Bloom, 2005). Unfortunately, modern agricultural systems are also highly inefficient in their N use, typically losing 50-70% of applied N to the environment (Coskun et al., 2017). Thus, understanding how plants sense and respond to N nutrient/metabolites is critical to enhance crop yield and improve N-use efficiency. Nitrate is the main source of N for plants in many natural as well as agricultural systems. Once inside the plant cells, nitrate can be reduced to nitrite and then to ammonium by the action of nitrate reductase (NR) and nitrite reductase (NIR), respectively (Crawford and Glass, 1998). In addition to its role as a nutrient, nitrate can act as a local and systemic signaling molecule modulating gene expression, metabolism, physiology, growth and developmental processes (Guan, 2017; Fredes et al., 2019). Nitrate sensing is mediated at least in part by the transporter and receptor NITRATE TRANSPORTER 1.1 (NRT1.1), also known as NPF6.3. NRT1.1 is required for nitrate signaling, which initiates early gene expression responses to nitrate for genes involved in nitrate transport, nitrate assimilation and signaling factors, among others. Since the signaling role of NRT1.1 appears to be independent from its transport activity,

it has been proposed as membrane transceptor with dual transporter/sensor function (Ho et al., 2009; Gojon et al., 2011). Downstream of NRT1.1, Ca^{2+} acts as a second messenger in the nitrate signaling pathway modulating the activity of endogenous Ca^{2+}-sensor protein kinases (CPKs) (Riveras et al., 2015; Liu et al., 2017). Specifically, CPK10, CPK30 and CPK32 have been proposed as activators of NIN-LIKE PROTEIN 7 (NLP7) an important transcription factor in the nitrate response (Marchive et al., 2013; Liu et al., 2017). In addition to NLP7, other regulatory proteins have been reported to mediate transcriptional responses to nitrate such as TGA1/TGA4 among others (Alvarez et al., 2014; Araus et al., 2016; Gaudinier et al., 2018).

Nitrate has been shown to control specific developmental processes both in root and shoot organs (Fredes et al., 2019). Nitrate releases seed dormancy leading to higher germination percentages for a wide variety of plant species (Alboresi et al., 2005; Duermeyer et al., 2018). Moderate nitrate availability can have a stimulatory effect on primary and lateral root lengths, while a severe deficiency as well as very high nitrate supply can inhibit both, lateral root branching and lateral root elongation (Sun et al., 2017). Nitrate signaling can increase root hair density in Arabidopsis presumably to increase nutrient uptake capacity (Canales et al., 2017). While high N concentrations delay flowering time, plants grown under low N accelerate flowering presumably to escape from unfavorable environmental conditions (Yuan et al., 2016; Gras et al., 2018). Induction of leaf growth by nitrate has been reported in many studies (Rahayu et al., 2005; Merigout et al., 2008). Nitrate-elicited shoot growth has been associated with translocation of root-derived cytokinin (CK) to the shoot (Takei et al., 2001; Takei et al., 2004; Poitout et al., 2018). In addition, nitrate-induced CKs can also act as long-distance signals in the control of the shoot apical meristem, increasing its size and flower production (Landrein et al., 2018). Specifically, Nitrate

treatment triggers apical meristem growth, a dose-dependent induction of WUSHEL (WUS) and a cytokinin reporter gene (pTCSn::GFP) (Landrein et al., 2018).

Leaf cells initially proliferate before transitioning to cell expansion and finally terminating growth (Andriankaja et al., 2012). The transition to postmitotic cellular expansion begins at the tip of the leaf and moves progressively from the tip to the base (Beemster et al., 2005; Gonzalez et al., 2012). Once cells cease proliferation, cells begin to expand mainly by cell wall loosening that continues to fuel further leaf growth (Cosgrove, 2016; Cosgrove, 2018). Thus, the overall change in organ size in a growing tissue over time depends on the balance between cell expansion and cell proliferation (Green, 1976). A large fraction of cells in leaf epidermis is generated through the stomatal lineage, in which cells divide asymmetrically to generate both pavement cells and stomatal cells (Bergmann and Sack, 2007). In principle, alterations of leaf size are thought to result from several factors that impact on rates of cell proliferation or cell elongation, duration of meristemoid division, extent of cell proliferation phase and number of founder cells incorporated into the primordium during its initiation in the shoot apical meristem (Powell and Lenhard, 2012; González and Inzé, 2015). Curiously, inhibition of cell division is often compensated by an induction in cell expansion, which often triggers strongly diminished whole organ size (Horiguchi and Tsukaya, 2011; de Veylder et al., 2011).

Cell expansion is often associated with a process known as endoreplication, which is characterized by repeated rounds of genome replication without subsequent mitosis (de Veylder et al., 2011). Endoreplication typically occurs in metabolically active and specialized cells. However, this process can also be observed in cells that do not match this description (Lee et al., 2010). A positive correlation between DNA content and cytoplasmic volume has been found in plant epidermal cells of diverse tissues, including leaves and sepals (Melaragno, 1993; Roeder et

al., 2010; Roeder et al., 2012; Katagiri et al., 2016; Robinson et al., 2018). The extent of ploidy-dependent cell size change varies between cell layers. Whereas pavement cell size increases linearly with ploidy levels, internal cells appear not to respond to DNA content (Katagiri et al., 2016). Endoreplication is a crucial process that maintains many cellular and physiological functions. For instance, endoreplication is required for maintenance of trichome identity and differentiation (Bramsiepe et al., 2010). Seed germination depends on endosperm, a polyploid tissue, used as an energy source for early stages of post-germination growth before the hetero-to-autotrophic transition. Rapid hypocotyl growth during early seedling establishment correlates with endoreplication (Berckmans et al., 2011). Additionally, endoreplication is affected by several external cues. Absence of light triggers a boost of the endoreplication cycle in *Arabidopsis thaliana* hypocotyls (Gendreau et al., 1997). Mutants in auxin signaling, biosynthesis and/or transport show a shift from mitosis to endocycle (Ishida et al., 2010) . Jasmonates (JAs) were also shown to inhibit endoreplication in a Coronatine Insensitive 1 (COI1)-dependent manner, arresting cells in G1 phase prior to S-phase (Noir et al., 2013). Cytokinin promotes the onset of endoreplication through upregulation of Cell Cycle Switch Protein 52 A1 (*CCS52A1*), an activator of an E3 ubiquitin ligase (Takahashi et al., 2013).

Cell cycle progression is coordinated by the activity of cyclin (CYC) and cyclin dependent kinase (CDK) complexes. CDK activity must reach two consecutive thresholds during the G1-to-S and G2-to-M transitions. The onset of endoreplication requires controlled inhibition of the CDK/CYC activity. Activity of these complexes is regulated at different levels: phosphorylation of CDK subunits, synthesis or proteolysis of phase-specific cyclins and CDK-specific inhibitors (CKIs) (Inzé and De Veylder, 2006). Three main levels of regulation have been associated to the endoreplication process. Firstly, transcriptional downregulation of premitotic/mitotic regulators.

Actually, transcript levels of mitotic CDK and cyclin genes decrease with the onset of endoreplication (Beemster et al., 2005). Secondly, G2-M-specific regulators are proteolytically controlled. Many mitotic cyclins are selectively promoted for destruction through ubiquitination by the Anaphase-promoting complex/Cyclosome (APC/C), which activity is determined by its association with activating subunits (Cebolla et al., 1999). A third mechanism by which CDK activity could be repressed is through the direct binding of CDK inhibitors (CKI). CDK inhibitor (CKI) CKI SIAMESE (SIM) is crucial for endoreplication and cell identity maintenance, which are in term required for Arabidopsis trichome formation. Another CKI is LOSS OF GIANT CELLS FROM ORGANS (LGO; also known as SIAMESE RELATED1, SMR1), which is required for high levels of endoreplication of pavement cells in leaves and sepals (Roeder et al., 2010). Cell size increases in a LGO dose-dependent manner in Arabidopsis sepal pavement cells (Robinson et al., 2018).

Despite manifest stimulation of plant growth by nutrients, many questions remain unanswered, particularly with regards to N nutrition: How is cell division or cell expansion controlled by plant N-nutritional status in shoots? How does nitrate nutrient modulate organ growth? How are these processes regulated and coordinated to reach a specific organ size? We address these questions using live-imaging, genomics and molecular genetic approaches. Our results indicate that external nitrate is sensed early after germination with an impact on endoreplication and cell expansion both in cotyledons and leaves in an LGO-dependent manner. We observed that organ size is determined by external nitrate concentrations, even when endoreplication is disrupted, due to the substitution by cell division. Our results provide a working model for how nitrate modulates shoot organ size as well as suggest nitrate interacts with an organ-level control mechanism to specify organ size.

Hypothesis

Nitrate regulates shoot growth through the modulation of endoreplication process in *Arabidopsis thaliana*.

General Aim

To identify the role of nitrate-mediated endoreplication process during shoot development.

Specific Aims

1.- To evaluate changes in cell area and ploidy levels in response to nitrate availability.

2.- To identify which cell cycle genes are modulating the nitrate-mediated endoreplication process.

3.- To identify the regulatory elements upstream of the cell cycle genes that control shoot growth in response to nitrate.

MATERIAL AND METHODS

Plant material and growth conditions

Arabidopsis thaliana Columbia (Col) accession was used as wild-type in all experiments. Seeds were sterilized with 50% chlorine solution for 7 minutes, washed five times with sterile distilled water and then placed on 30 mL of agar medium in a 35-mm petri dish. Plants were grown under long-day photoperiods (16 h light 22ºC/ 8h dark 22ºC) at 260 μmol $m^{-2}s^{-1}$ light intensity using T8 Philips Standard lamps 17-W for in vitro plant growth. All plants were grown in a N-free basal Murishage and Skoog (MS) agar medium supplemented with 5 mM KNO_3, 0.5 mM KNO_3, 5 mM KNO_3, 0.25 mM Glutamine, 2.5 mM Glutamine, 0.25 mM Ammonium succinate or 2.5 mM Ammonium Succinate as N-sources.

lgo-2 (Roeder et al., 2010), *chl1-5* (Alvarez et al., 2014), *nlp7-1* (Liu et al., 2017), *krp1/2/5/6/7* (*ick1/2/4/6/7*) (Cheng et al., 2013) were described elsewhere. Reporter lines such as pAR169/pAR229 (Roeder et al., 2010) and pAR181 (*pML1::H2B-mGFP*) (Roeder et al., 2010) were described elsewhere. pDR67 (*pLGO::3XVENUS-N7*) reporter line was created by LR recombination of pAR334 (3X Venus N7 in the pENTR D TOPO vector) into pAR242 (pMLBART vector with LGO promoter and terminator flanking the gateway site). The pAR334 (3XVenus-N7 in pENTR D TOPO) plasmid was created by PCR amplifying 3XVenus-N7 from -60 3XVenus-N7 BJ36 (Roeder et al., 2012) with oAR646 and oAR647 and cloning the product into pENTR D TOPO (ThermoFisher). The pAR225 plasmid (LGO promoter-EcoRV-LGO 3'region) was created by PCR amplifying the LGO promoter with oAR476 and oAR479, the LGO 3' region with oAR478 and oAR477, fusing the two products through overlap extension PCR and cloning the full-length fusion into pGEM Teasy (Promega). The Gateway Conversion RFB (TermoFisher) with Not I site removed was blunt end cloned into the EcoRV site of pAR225 to

create pAR241 (LGOp::GW-LGO-3'region). pAR241 was cut with Not I and cloned into pMLBart to create pAR242 (LOGp::GW-LGO 3'region in a binary vector conferring BastaR) pDR67 pLGO::3XVenus-N7 was transformed into WT Col by Agrobacterium-mediated floral dipping, and successful transformants were selected with BASTA. All new vectors were verified by sequencing before plant transformation. To track nuclei and cell boundaries in *lgo-2* mutant plants, pAR169/pAR229 was crossed to *lgo-2* and mutants carrying both transgenes were selected in the F2.

Vegetative area measurement

Plants were grown horizontally in square plates. Plates were then scanned at 700 dpi in TIFF format using HP scanner. Vegetative area was quantified using ImageJ software (https://imagej.nih.gov/ij/).

RNA-Seq library construction and data analysis

To perform RNA-seq approach, RNA was extracted from ~20 mg shoot tissue and used for Illumina compatible library preparation of three biological replicates from 3 DAS plants grown under three contrasting nitrate conditions (0, 0.5 or 5 mM). Total RNA was extracted using PureLink™ RNA mini kit (Invitrogen) according to the manufacture's instructions. RNA integrity and concentration were determined with Fragment Analyzer System (Agilent) and NanoDrop™ 2000 (Thermo Fisher Scientific), respectively. cDNA libraries were created with Illumina TruSeq Stranded mRNA Library prep kit according to manufacturer's instructions. Then, cDNA libraries were sequenced on Illumina HiSeq 2500 v4 platform (100 pb paired-end reads). The resulting reads were mapped to *A.thaliana* Col-0 Reference Genome TAIR 10 using Tophat software. The read counts for each gene was calculated using Rsubread R package, and DESeq2 was used to

identify differentially expressed genes (DEGs) using log2 > 0.7 and *p*-value < 0.01 as significant cutoff.

Gene ontology (GO) enrichment analysis of DEGs was performed with agriGO V2 analysis toolkit (http://bioinfo.cau.edu.cn/agriGO/) to determine the significantly enriched GO terms. A significant *p*-value < 0.05 was used to identified enriched terms. The top 10 GO terms with lowest *p*-values were selected for Table 1.

Transcriptional reporter of LGO

Spatial expression of *LGO* in cotyledon cells was achieved using the transcriptional reporter *pDR67* (*pLGO::3XVENUS-N7*). To observe cells expressing the transcriptional reporter, we analyzed cotyledons from plants grown in 0 or 5 mM nitrate. Then, plants were submerged in Propidium Iodide (PI) solution (10 mg/ml) for 5-10 min and then mounted with a cover slip. The resulting images were cropped with ImageJ to remove transcriptional reporters expressed beyond cotyledons. Plants were imaged at 3 DAS with Zeiss 710 confocal laser scanning microscope with a 20X water-immersion objective. Seedlings were excited with an argon laser (514 nm). Images were then segmented with the Constanza (CONstanza STack ANalZer Application) ImageJ plugin (http://www.plant-image-analysis.org/software/costanza), providing high-resolution three-dimensional segmentation of nuclei expressing the transcriptional reporter *pLGO::VENUS-N7*. Constanza-segmented images were used to calculate the number of cells expressing *LGO* per cotyledon. Cell expressing *LGO* beyond cotyledons were excluded from this analysis.

Cotyledon live-imaging

Wild-type and *lgo-2* plant cotyledons were imaged by confocal imaging. Both plasma membrane and nuclei were tracked using the vectors pAR169 and pAR229 (*pML1::mCitrine-RCI2A* and *pML1::H2B-mTFP* respectively) according to Roeder et al. (2010). The same region of cotyledon cells was imaged every 24 hours from 3 to 7 DAS. Three-dimensional optical z-stacks were collected with a Zeiss 710 confocal laser scanning microscope using a 20X water-immersion objective (NA=1.0). Samples were excited with an argon laser (458 nm: 4.5% and 514: 0.8%). An accurate analysis was achieved with Z-section of 2.5 µm. The resulting confocal stacks were converted from LSM to TIFF image stacks using FIJI (http://fiji.sc/Fiji) and imported into MorphographX for segmentation and analysis (Barbier de Reuille et al., 2015). The mCitrine and mTFP channels were split and both stacks were loaded into the software. The stacks were processed (Gaussian blur, edge detect and fill holes) to obtain the outline of cotyledon adaxial epidermal cells. The surface was generated with a polygonal mesh using 5 µm cubes. The mesh was subdivided and subsequently smoothed twice until obtain ~500,000 vertices. Individual cells were manually seeded and segmented using the watershed algorithm. Cell lineages were defined manually by matching mother and daughter cell labels over time using the parent labels function. Heatmaps were generated to visualize the aereal growth and proliferation rate. We defined cumulative cell growth as lineage area at a specific time relative to lineage area at the first-time point (3 DAS). Cell division rate was defined as the ratio of the number that divided from specific time-point to the number of cells at the beginning of time-course analysis (3 DAS).

For nuclear size analysis, mTFP channel was loaded into MorphographX software for stack processing (Brighten/Darken, Gaussian blur , Binarize stack = 10.000, Remove noise). Mesh were

generated using 1 μm as a cube size. Finally, nuclei were seeded and segmented individually using watershed algorithm. Nuclei size analysis was conducted through the Heatmap function.

Flow cytometry analysis.

For each genotype, approximately 30 cotyledons (7 DAS) and 10 leaves (15 DAS) were chopped with a razor blade in 600 μl Aru buffer (Arumuganathan and Earle, 1991) from plants grown under different nitrogen concentrations. The suspension was filtered through a 30 μm nylon mesh (Sigma-Aldrich), followed by incubation with 50 μg/ml DNase-free RNase and 1 μg/ml PI (Sigma-Aldrich). Flow cytometry was conducted using the Accuri™ C6 Plus (Becton Dickinson) or FACSCanto II (Becton Dickinson). To distinguish internal from epidermal cell ploidy, epidermal nuclei were identified with the reporter line *pAR180* (*pML1::H2B-mGFP*). Plants were chopped, filtered and stained as mentioned above. At least 5000 nuclei were counted per sample. Histograms of the PI fluorescence for each population showed the relative DNA content of each population. Each experiment was repeated at least three times using similar number of nuclei.

Primer Table

name	sequence	purpose
oAR646	caccggtaccaaaATGGTGAGCAAGGGCGAGGAG	Amplify Start of 3XVenus with KpnI site
oAR647	CTCTAGaTTACTCTTCTTCTTGATC	Amplify end of N7 with stop and XbaI site.
oAR476	GCGGCCGCcttgatccttatcacctaaacgaaccaaac	PCR start of LG promoter with Not I site
oAR477	GCGGCCGCtgttgcttattggatgagttgcgtagaca	PCR end of LGO 3' region with Not I site
oAR478	aacaaaaacatacacaagtttagaGATATCggcttaattcaatatttacatt	PCR start of LGO 3'region with EcoRV and LGOp overhang
oAR479	aatgtaaatattgaattaagccGATATCtctaaacttgtgtatgtttttgtt	PCR end of LGO promoter EcoRV with overhang of 3' region

RESULTS

AIM 1

Nitrate signaling is important for shoot growth early after germination.

It is well documented N nutrient/metabolites stimulate shoot growth and development (Liu et al., 2017; Rahayu et al., 2005; Pitout et al., 2018). As a first step to address the mechanism involved in nitrate control of shoot growth, we measured shoot area from plants grown in agar plates with 0, 0.5 or 5 mM nitrate as the only nitrogen source. For the first 3 days after sowing (DAS), plants germinated, cotyledons opened, and expanded similarly under the three N conditions. This result is consistent with early post-germination growth being supported primarily by N-reserves in the cotyledon with no phenotypic impact of external N sources at this stage (Figure 1A and 1B). However, the plant growth rate was clearly affected by exogenous N shortly afterwards, with significant differences in shoot size as early as 4 days after germination which became larger over time in contrasting N conditions (Figures 1A and 1B). By 7 DAS, plants under 5 mM nitrate grew approximately 4-fold more than those growing without a N source (Figure 1B).

We then evaluated whether induction of post-embryonic growth was a general effect of a N source or a nitrate-specific effect. We performed a new experiment with plants grown with the same molar concentration of N but using glutamine or ammonium as the only N-sources. (Figure 1C). We observed post-embryonic shoot growth was not promoted by these other N sources, growth was promoted only in the presence of nitrate under our experimental conditions. In addition to nitrogen, we assessed weather carbon availability could also impact post-embryonic plant growth under the same experimental conditions. However, we observed vegetative area was not affected by increasing sucrose in the media (Figure 2). These results support the exclusive role of nitrate during post-embryonic plant growth under our experimental conditions.

To test whether nitrate signaling was required for post-germination nitrate-elicited growth, we quantified vegetative area in mutants of key components of the known nitrate signaling pathway. Mutant plants in the nitrate sensor NRT1.1/NPF6.3 (*chl1-5* mutant lines) were significantly smaller as compared to WT plants 7 DAS in the presence of nitrate (Figure 1D). We then asked whether NLP7, a key transcription factor in the primary nitrate response downstream of NRT1.1, was also implicated in the observed nitrate-mediated shoot growth. We compared vegetative area in *nlp7-1* mutant and wild-type plants grown under 0, 0.5 or 5 mM nitrate. Similar to the phenotype for *chl1-5* plants (mutant in sensing and nitrate transport), we observed *nlp7-1* mutant plants were significantly smaller than wild-type plants 7 DAS in the presence of nitrate (Figure 1E).

These results indicate nitrate signaling via NRT1.1/NLP7 contributes to modulating shoot growth as early as 7 DAS. While earlier growth is probably supported by seed reserves, nitrate sensing via NRT1.1 and NLP7 is required for normal shoot growth early after germination.

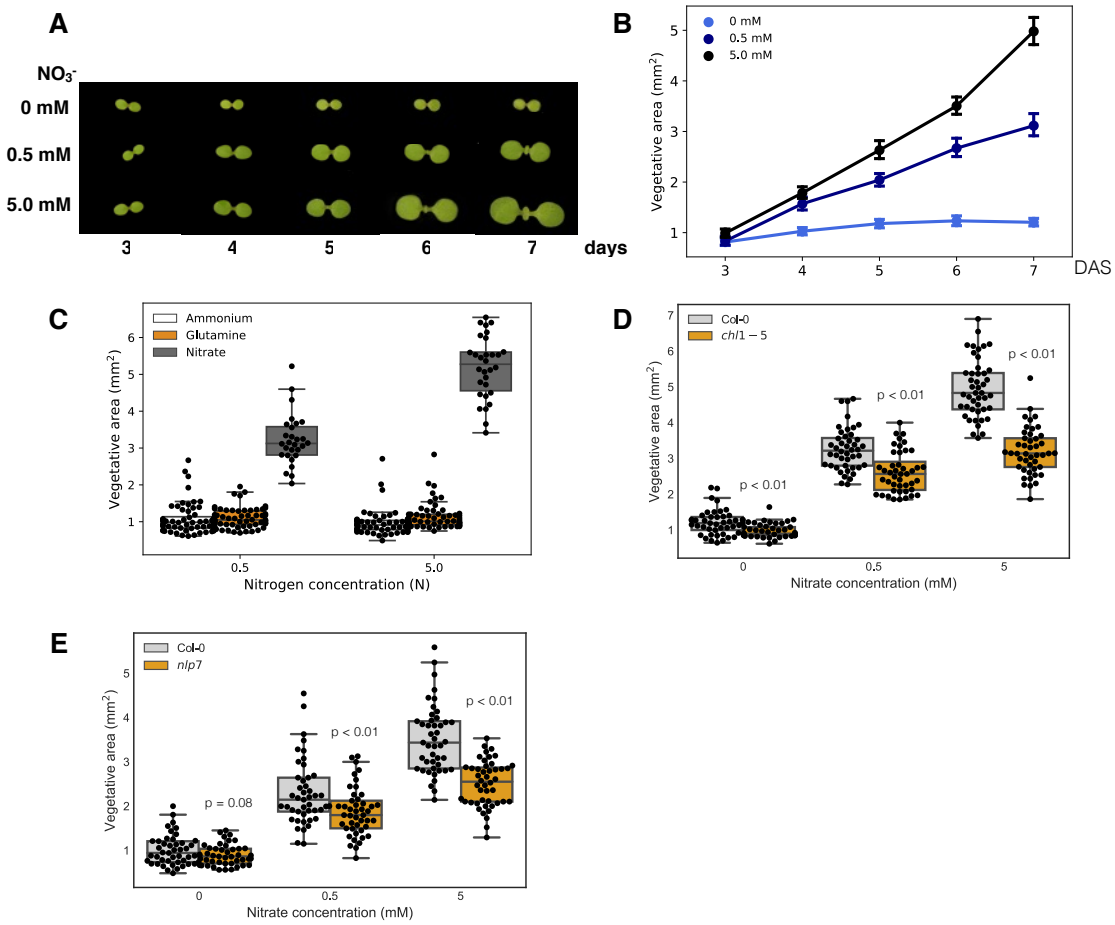

Figure 1 | Nitrate modulates shoot growth shortly after germination.
(A) Plants were grown under different nitrate concentrations (0 mM, 0.5 mM and 5.0 mM) and photographed from 3 to 7 DAS.
(B) Graph showing average vegetative area from plants grown under three nitrate conditions. Bars denote standard error. n = 45 seedlings each point.
(C) Boxplot showing vegetative area from WT plants grown with different N sources at 7 DAS: Glutamine, Ammonium Succinate and Nitrate. Same molar concentration of nitrogen was used for each N source. Vegetative area was compared for each concentration between different nitrogen sources.
(D) Measurements of vegetative area in *chl1-5* (NRT1.1 null-mutant) and wild-type plants grown in different nitrate concentrations (0, 0.5 and 5 mM) at 7 DAS. Statistically significant differences between genotypes are indicated (t-test). n = 45 seedlings for each box-plot. At least three biological replicates were repeated for each experiment.
(E) Measurements of vegetative area in *nlp7-1* and wild-type plants grown in different nitrate concentrations (0, 0.5 and 5 mM) at 7 DAS. Statistically significant differences between genotypes are indicated (t-test). n = 45 seedlings for each box-plot. At least three biological replicates were repeated for each experiment. Data were compared using Student's tests for each nitrate concentration.

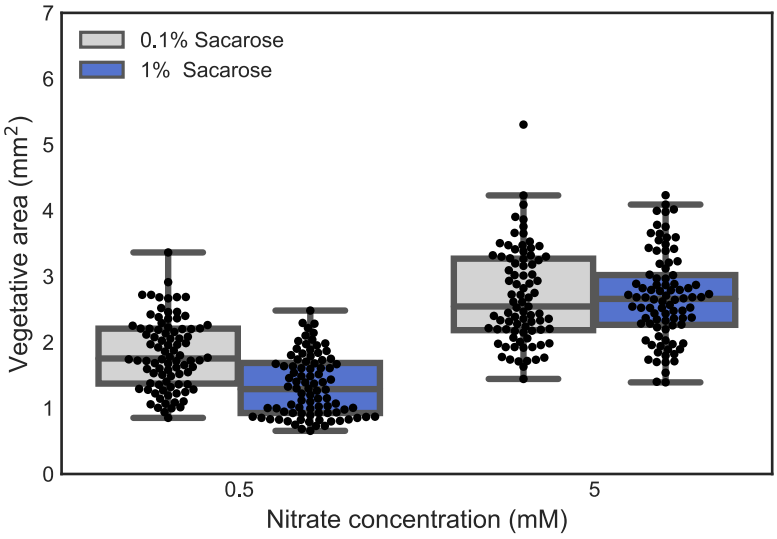

Figure 2 | Nitrate post-embryonic growth is exclusively triggered in response to nitrate. Boxplot showing the role of sucrose increment during post-embryonic growth. 0.1 and 1% of sucrose were used with different concentration of nitrate and vegetative area was quantified at 7 DAS.

Cell expansion plays an important role in nitrate-mediated cotyledon growth.

Shoot growth is supported by coordinated cell proliferation and cell expansion. We asked whether any of these developmental processes were regulated by nitrate during post-embryonic growth. Epidermal cells of cotyledons from plants grown under different nitrate concentrations (0 or 5 mM) were tracked from 3 to 7 DAS. The same cotyledon spot was imaged every 24 h during this five-day period. The double reporter *pATML1:: mCitrine-RCI2A* and *pATML1::H2B-mTFP* (pAR169/pAR229) was used to track cell boundaries and nuclei respectively (Roeder et al., 2010). MorphographX software was used for cell and nuclei segmentation and to calculate growth properties for each cell lineage (Barbier de Reuille et al., 2015). The epidermis is thought to be a major driver of leaf growth (Savaldi-Goldstein et al., 2007; Hong et al., 2016). So that we could consider the growth of the predominant epidermal cell type: pavement cells. Thus, stomatal cell lineages were excluded from our analysis. In order to remove undifferentiated pavement cells and stomatal cell lineages, cells with cell area below an established threshold were filtered out for each time-point (Figure 3B and 3D). Cell growth and cell division were analyzed for the same group of epidermal cells (Figures 3A-3D; 4A-4B; n = 164 cell lineages in 5 mM nitrate, 244 cell lineages in 0 mM nitrate). Cumulative cell growth and cell division were calculated as a ratio of value at specific time-points in comparison with the starting point of our time-course analysis 3 DAS. We observed that epidermal cells from plants grown in the absence of nitrate expanded marginally by the end of the time-course. (Figure 3B, 3E and 3F). In contrast, 5 mM nitrate supply significantly increased cell size approximately 4-fold during this cotyledon live-imaging time-course experiments (Figure 3D, 3E and 3F).

Leaf development initiates with a cell proliferation phase that is followed by cell expansion that starts at the tip of the leaf (Andriankaja et al., 2012). In cotyledons, about 30% of cells have divided by day 3, after which cell proliferation is not detected (Tsukaya et al., 1994; Stoynova-Bakalova et al., 2004) . Consistent with these previous reports, we did not observe cell division in pavement cells of the cotyledon during the time-course analysis under our experimental conditions (Figure 4A-4B). These results are consistent with post-embryonic cotyledon growth explained mainly by cell expansion in response to nitrate supply.

Cell-to-cell size variability has been described in many plant tissues including meristem cells and epidermal cells of sepals and leaves (Kheibarshekan Asl et al., 2011; Elsner et al., 2012; Kierzkowski et al., 2012; Tauriello et al., 2015). We inquired whether cell-to-cell size variability is influenced by plant nutritional status in cotyledons. We used the coefficient of variation (CV) to quantify cell size variability of cotyledon epidermal cells (Uyttewaal et al., 2012; Hong et al., 2018). As expected, we did not observe significant differences in cell size variability at the beginning of our experiment 3 DAS for different nitrate concentrations (Figure 4C). However, epidermal cell size heterogeneity was significantly higher in the presence of 5 mM nitrate 7 DAS (Figure 3G). Our results show that nitrate-elicited cell expansion triggers a switch from a homogenous to heterogeneous cell area state.

Based on these results, we conclude that post-embryonic cotyledon growth induced by nitrate supply is explained by cell expansion. Moreover, nitrate-elicited cell expansion is not uniform across cells in defined tissues such as the epidermis, as indicated by heterogeneous cell size after expansion has initiated. Our results also highlight nitrate-mediated cotyledon growth as a good model system to understand cell expansion dynamics to achieve organ growth in Arabidopsis.

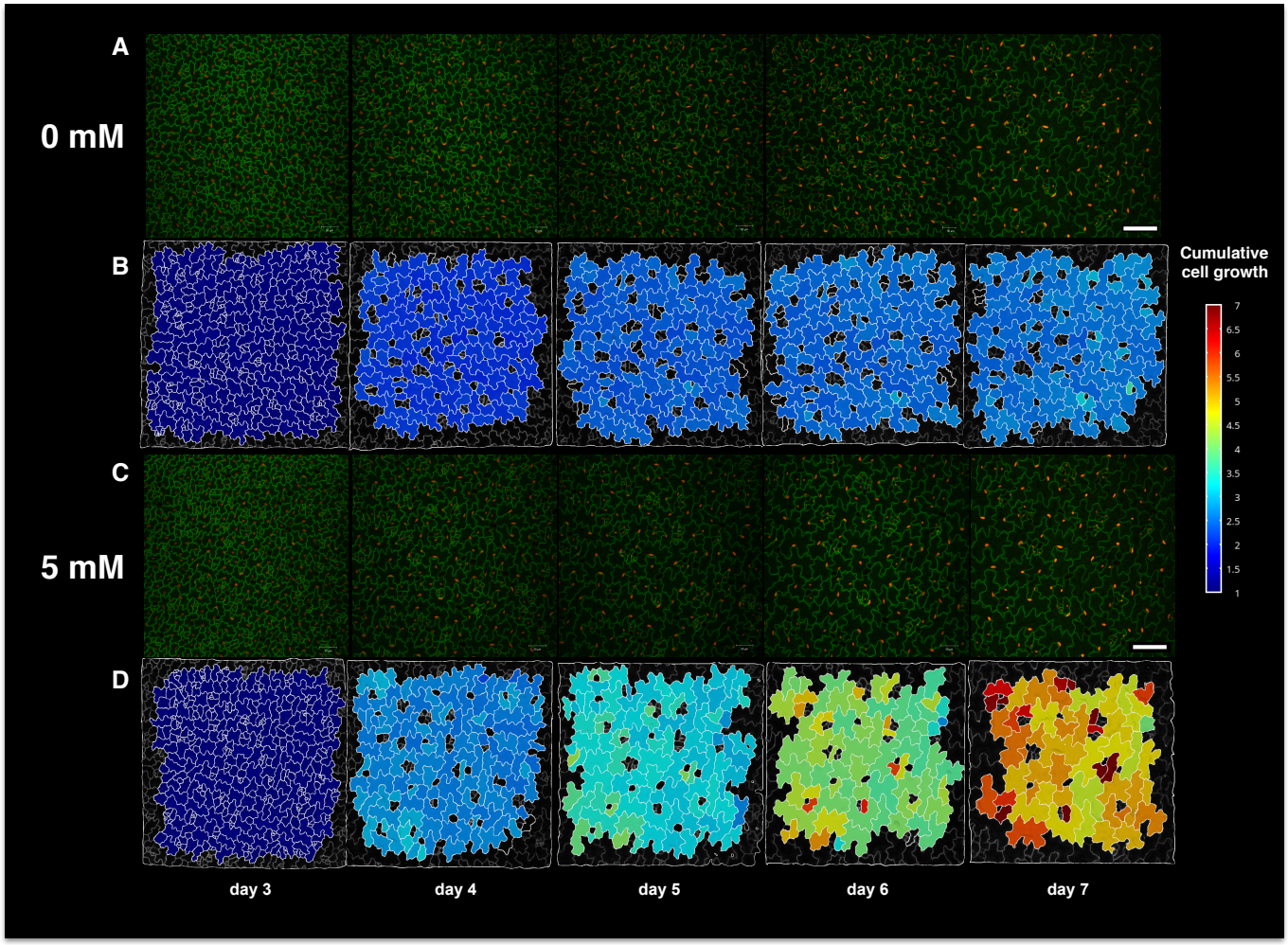
A
0 mM
B
C
5 mM
D
Cumulative cell growth
7
6.5
6
5.5
5
4.5
4
3.5
3
2.5
2
1.5
1
day 3
day 4
day 5
day 6
day 7

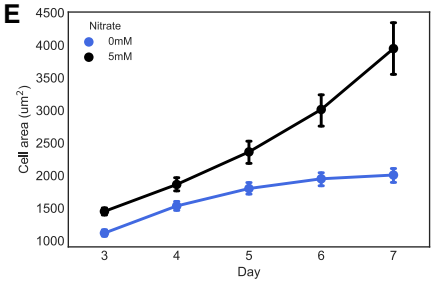
E
Nitrate
0mM
5mM
Cell area (um²)
4500
4000
3500
3000
2500
2000
1500
1000
3
4
5
6
7
Day

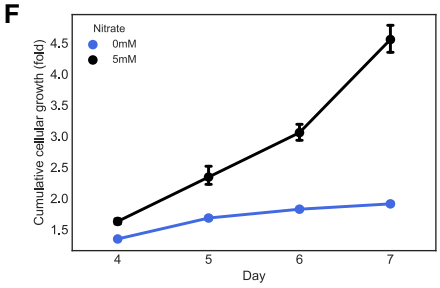
F
Nitrate
0mM
5mM
Cumulative cellular growth (fold)
4.5
4.0
3.5
3.0
2.5
2.0
1.5
4
5
6
7
Day

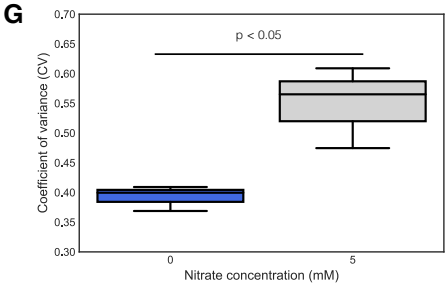
G
p < 0.05
Coefficient of variance (CV)
0.70
0.65
0.60
0.55
0.50
0.45
0.40
0.35
0.30
0
5
Nitrate concentration (mM)

Figure 3 | Nitrate-mediated growth in Arabidopsis cotyledons is mediated by cell expansion.
(A and C) Confocal stack maximum-intensity projections of wild-type cotyledons from plants grown in two contrasting nitrate concentrations (0 or 5 mM). Epidermal cells are labeled in green with the reporter *pATML1::mCitrine-RCl2A*. Nuclei were labeled in red with reporter *pATML1::H2B-mTFP*. Epidermal cells of cotyledons were imaged every 24 hours from 3 to 7 DAS.
(B and D) Heatmap of cumulative growth in cellular area from cotyledon of wild-type plants grown in 0 mM (B) or 5 mM (D) nitrate. Cumulative growth is calculated as the area of the cell at the time point indicated divided by the area of the same cell at day 3. Some cells shown in a previous time-point are not shown in the next time-point because cells grown out of the observation frame.
(E) Average pavement cell area for three biological replicates in wild-type plants grown in contrasting nitrate conditions as indicated before for (A) and (C). 244 and 164 cell lineages were tracked in 0 and 5 mM respectively. Stomata cell lineage were filtered from the analysis.
(F). Cumulative cellular growth calculated as the ratio of cell area at specific times (4, 5, 6 or 7 DAS) and the starting point of the time-course analysis (3 DAS).
(G) Coefficient of variance (CV) was used to estimate cell area heterogeneity in pavement cells of the Arabidopsis cotyledon from three biological replicates (t-test) at 7 DAS. CV was calculated as the ratio of standard deviation and average cell area. Epidermal cells were segmented and analyzed with MorphographX software (Barbier de Reuillie et a., 2015). Scale bars, 100 µm

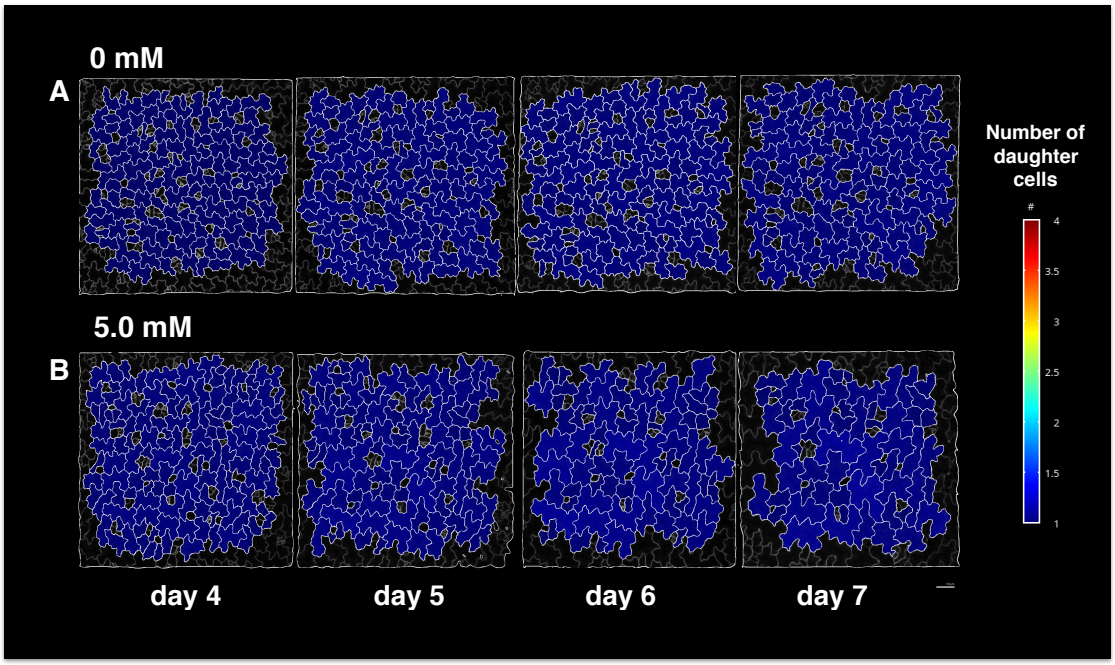

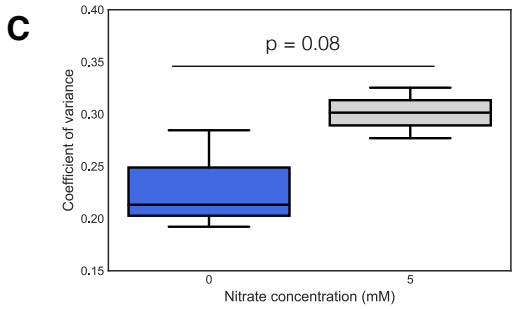

Figure 4 | Nitrate post-embryonic growth is exclusively triggered by cell expansion.
(A and B) Heatmap of cell proliferation rate of wild-type cotyledons. Confocal stack maximum-intensity projection images of wild-type plants grown in two different nitrate concentrations (0 mM or 5 mM). Epidermal cells were segmented and tracked with MorphographX software. Note the cells in which divisions are detected are in the stomatal lineage.
(C) Coefficient of variance (CV) was used to estimate cell area heterogeneity in pavement cells of the Arabidopsis cotyledon from three biological replicates (t-test) at 3 DAS. CV was calculated as the ratio of standard deviation and average cell area. Epidermal cells were segmented and analyzed with MorphographX software (Barbier de Reuillie et a., 2015). Scale bars, 100 µm.

Nitrate sensing promotes cell expansion through endoreplication.

A positive correlation has been described between cell size and DNA content in different plant cell-types (Melaragno, 1993; Roeder et al., 2010; Katagiri et al., 2016). Since cell expansion without division is a characteristic of endoreplication, we asked whether endoreplication is also regulated by nitrate availability. We performed flow-cytometry analysis to assess ploidy profiles in cotyledons from plants grown under 0, 0.5 or 5 mM nitrate as the only nitrogen source. We observed DNA content increased with nitrate concentration in cotyledons (Figures 5A). In the absence of nitrate, 2C and 4C were the predominant ploidy levels of the cotyledon (Figure 5C-D). In contrast, nuclei from plants grown in 0.5 or 5 mM nitrate showed a significant increase in endoreplication as compared to nuclei from plants grown with 0 mM nitrate (Figure 5C-D). In order to evaluate the developmental component for endoreplication, ploidy profiles were also measured in cotyledons from plants grown in different nitrate conditions 3 DAS (Figure 6). Interestingly, we did not observe significant differences in ploidy in cotyledons from plants grown in different nitrate concentrations 3 DAS, consistent with our observation that there are no differences in growth at this stage (Figure 1B). We next asked whether the NRT1.1/NLP7 signaling pathway was also necessary for nitrate-elicited endoreplication events. Ploidy profiles of DNA content were analyzed in *chl1-5* and *nlp7-1* mutant and wild-type plants. We observed that both NRT1.1 and NLP7 were required to reach higher ploidy levels during nitrate-elicited growth as compared to wild-type plants (Figure 5F-5G). These results indicate that key nitrate signaling regulators contribute to nitrate-mediated endoreplication during post-embryonic growth.

We next asked whether the impact of nitrate on endoreplication is restricted to specific cell-types or can be observed in different tissues of the cotyledon. Using a nuclear-localized epidermal-specific reporter *pATML1::H2B-mGFP* (Roeder et al., 2010), we assessed DNA content in

cotyledon epidermal cells (GFP-positive) and internal cell layers (GFP-negative) from plants grown under 0, 0.5, or 5 mM nitrate. In both epidermal and internal cells, nitrate increased endoreplication, indicating nitrate regulates endoreplication in different cell-types (Figures 5C and 5D).

Then, we evaluated whether nitrate can impact endoreplication in true leaves. We conducted a flow-cytometry analysis in the first pair of true leaves from plants grown in 0.5 or 5 mM nitrate concentration for 15 days. Similar to cotyledons, the first true pair of true leaves also showed higher-order ploidy values correlating with nitrate concentration (Figure 5B and 5E), which confirms endoreplication as a general response to nitrate availability during plant shoot growth.

Finally, in order to complement flow cytometry analysis, we asked whether epidermal nuclei area obtained from confocal images increased in response to nitrate because nuclear size correlates with DNA content in Arabidopsis (Jovtchev et al., 2006). Using the same nuclei epidermal reporter pATML1::H2B-mTFP used for cotyledon live-imaging (Figure 2), we evaluated the epidermal nuclear area distribution from cotyledons of plants grown under 0 or 5mM nitrate (Figure 7A and 7B). We observed that nuclei from plants grown in the absence of nitrate were significantly smaller than epidermal nuclei from plants grown under 5 mM nitrate (Figure 7B and 7C).

Exogenous nitrate supply promotes endoreplication in cotyledons and true leaves, both in epidermal and internal cell-layers. Key nitrate-responsive factors such as NRT1.1 and NLP7 are required to reach proper DNA content and cell size for nitrate-elicited leaf growth. Our results indicate nitrate signaling promotes endoreplication and cell expansion during cotyledon and leaf growth in *Arabidopsis thaliana*.

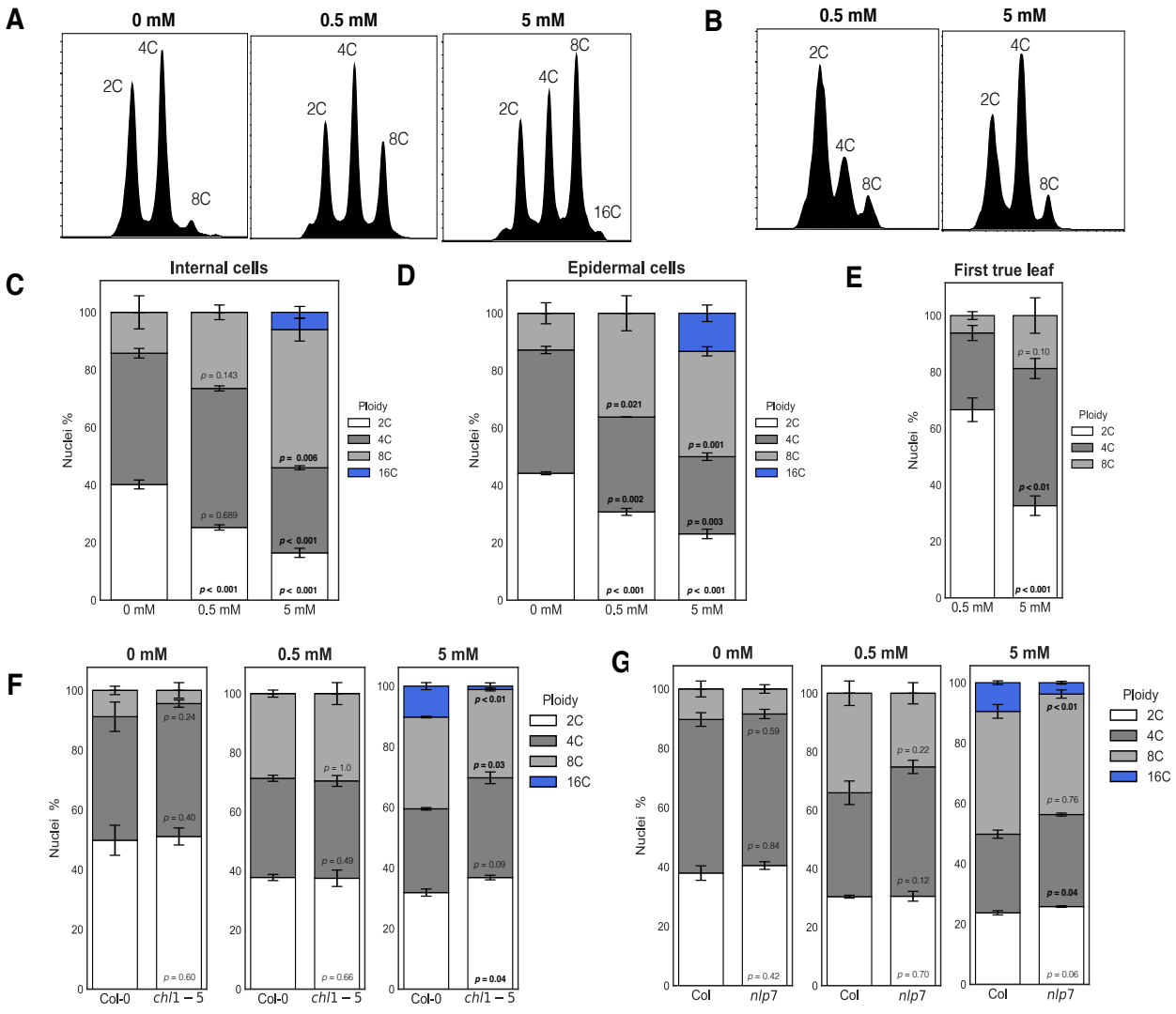

Figure 5 | Nitrate promotes endoreplication on different cell layers.
(A) Representative ploidy profile obtained by flow cytometry analysis of wild-type cotyledons 7 DAS. Plants were grown in three contrasting nitrate concentrations (0, 0.5 or 5 mM).
(B) Representative ploidy profile obtained by flow cytometry analysis of first pair of leaves 15 DAS. Plants were grown in 0.5 or 5.0 mM nitrate.
(C) Ploidy distribution of cotyledon internal cells from wild-type plants grown in 0, 0.5 or 5 mM nitrate at 7 DAS. The epidermal reporter *pATML1::H2B-mGFP* (pAR180) lines were stained with propidium iodide (PI) to separate internal from epidermal cells. At least three replicates were conducted for each experiment. Significant difference was detected by t-test analysis for each ploidy compared to 0 mM ($p < 0.05$).

(D) Ploidy distribution of cotyledon epidermal cells from wild-type plants grown in 0, 0.5 or 5 mM nitrate at 7 DAS, separated from the internal cells shown in C. At least three replicates were conducted for each experiment. Bars denote standard error of the mean in all stacked graphs. Significant difference was detected by t-test analysis for each ploidy compared to 0 mM ($p < 0.05$).
(E) Ploidy distribution of first pair of true leaves from wild-type plants grown in 0.5 or 5 mM nitrate at 15 DAS.
(F) Ploidy distribution in cotyledons from wild-type or *chl1-5* plants grown in 0, 0.5 and 5 mM nitrate 7 DAS.
(G) Ploidy distribution in cotyledons from wild-type or *nlp7-1* plants grown in 0, 0.5 and 5 mM nitrate 7 DAS. Significant differences were detected by t-test analysis for each nitrate concentration ($p < 0.05$).

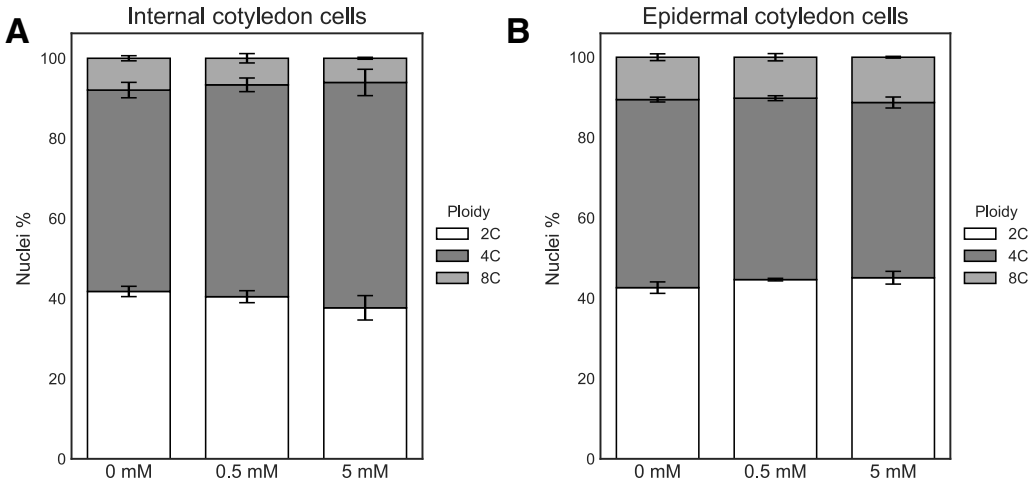

Figure 6 | Nitrate signaling controls post-embryonic endoreplication of cotyledons after day 3.

(A) Flow cytometry analysis of DNA content of internal cells from cotyledons of wild-type plants grown in different nitrate concentration at 3 DAS.

(B) Flow cytometry analysis of DNA content of epidermal cells from cotyledons of wild-type plants grown in different nitrate concentration at 3 DAS. The epidermal reporter *pATML1::H2B-mGFP* (pAR180) was stained with propidium iodide (PI) to separate internal from epidermal cells.

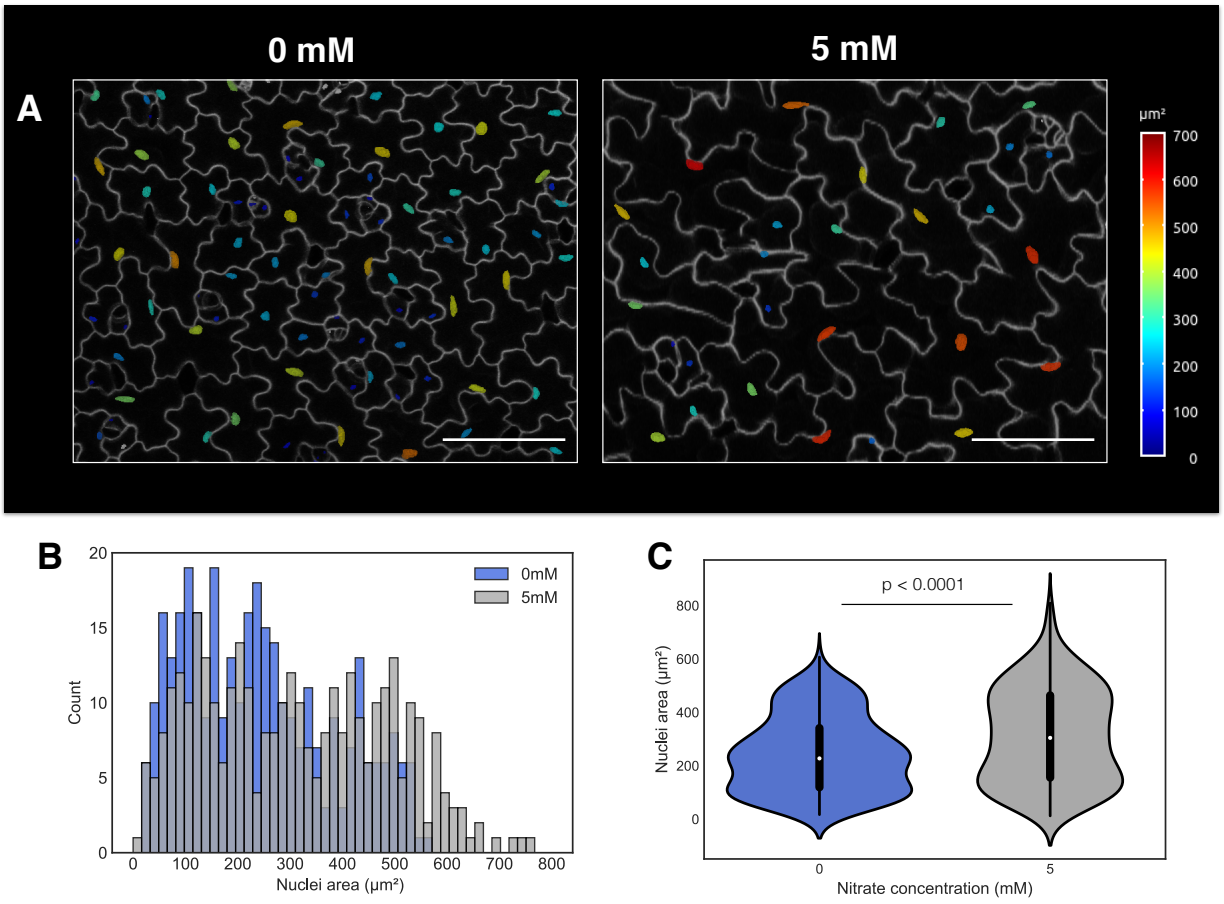

Figure 7 | Epidermal nuclei area is regulated in response to nitrate availability.
(A) Heat-map of epidermal nuclei area from cotyledon of wild-type plants grown in 0 or 5 mM nitrate at 7 DAS. Nuclei segmentation was conducted using MorphographX software (Barbier de Reuillie et al., 2015).
(B) Epidermal nuclei area distribution from cotyledon of wild-type plants grown in 0 or 5 mM nitrate 7 DAS. 338 epidermal nuclei were used for each concentration from three biological replicates.
(C) Epidermal nuclei area data used in (C) represented through a violin plot. All nuclei from epidermal cells were included in the analysis Significant difference was detected by t-test analysis. White dots indicate median values. The ends of the black boxes are the upper and lower quartiles. Scale bars, 100 μm

AIM 2

Nitrate-responsive genes during post-embryonic plant growth.

Most transcriptome analyses of the nitrate response have been performed at later developmental stages than those used here (Alvarez et al., 2014; Liu et al., 2017; Varala et al., 2018). In order to identify potential regulatory factors involved in nitrate-elicited post-embryonic cotyledon expansion and leaf growth, we performed a transcriptome analysis in shoots from plants grown with either 0 or 5 mM nitrate as the only nitrogen source (Figure 8A). We chose to carry out the analysis 3 DAS, before any phenotypic differences were observed, to detect early events as well as to avoid the confounding effect of developmental shifts. Interestingly, even at early developmental stages (3 DAS) we observed 1145 genes differentially expressed in response to external nitrate concentration in plant shoots (data not shown). In addition, many nitrate-responsive key elements that have been previously described within the nitrate signaling pathway in other tissues or developmental stages were found regulated under these experimental conditions, including *BT1*, *BT2* and *TGA1* (Alvarez et al., 2014; Araus et al., 2016).

Differentially expressed genes were classified using Gene Ontology (GO) terms and over-represented terms were identified using standard procedures (Tian et al., 2017). We found over-represented processes that have been described as important processes during post-embryonic growth such as lipid localization, cell wall organization, among others (Table I). Breakdown and remobilization of storage lipids are necessary for the heterotroph to autotroph transition in plants (Martin et al., 2002; Fait et al., 2006). On the other hand, regulation of cell wall components can modify the polysaccharide network affecting cell wall mechanical properties necessary for cell expansion.

In order to identify candidate regulatory genes in the context of this study, we focus our analysis on cell-cycle functions (Figure 8B). We found only one core cell-cycle gene with differential expression levels of mRNA in shoots 3 DAS when comparing 0 and 5 mM external nitrate concentration. The CDK inhibitor LGO was found differentially expressed with higher levels of expression under 5 mM nitrate as compared to 0 mM nitrate (Supplementary Table I). LGO encodes a cyclin dependent kinase inhibitor (CKI) that supports endoreplication and cell size identity during sepal development (Roeder et al., 2010).

Our results indicate external nitrate supply can trigger genome-wide expression changes as early as 3 days after germination in Arabidopsis plants. Moreover, our analysis suggest LGO may be implicated in nitrate-elicited growth early after germination.

Table 1. Over-represented Gene Ontology terms in response to nitrate 3 DAS.

Over-represented terms	**p-value**
response to stimulus	2.00E-27
response to chemical stimulus	5.00E-25
lipid localization	**1.30E-19**
response to stress	4.10E-18
response to oxidative stress	2.00E-14
plant-type cell wall organization	**1.20E-13**
secondary metabolic process	6.10E-13
phenylpropanoid metabolic process	8.60E-12
cellular amino acid derivative metabolic process	6.60E-11
phenylpropanoid biosynthetic process	8.50E-11

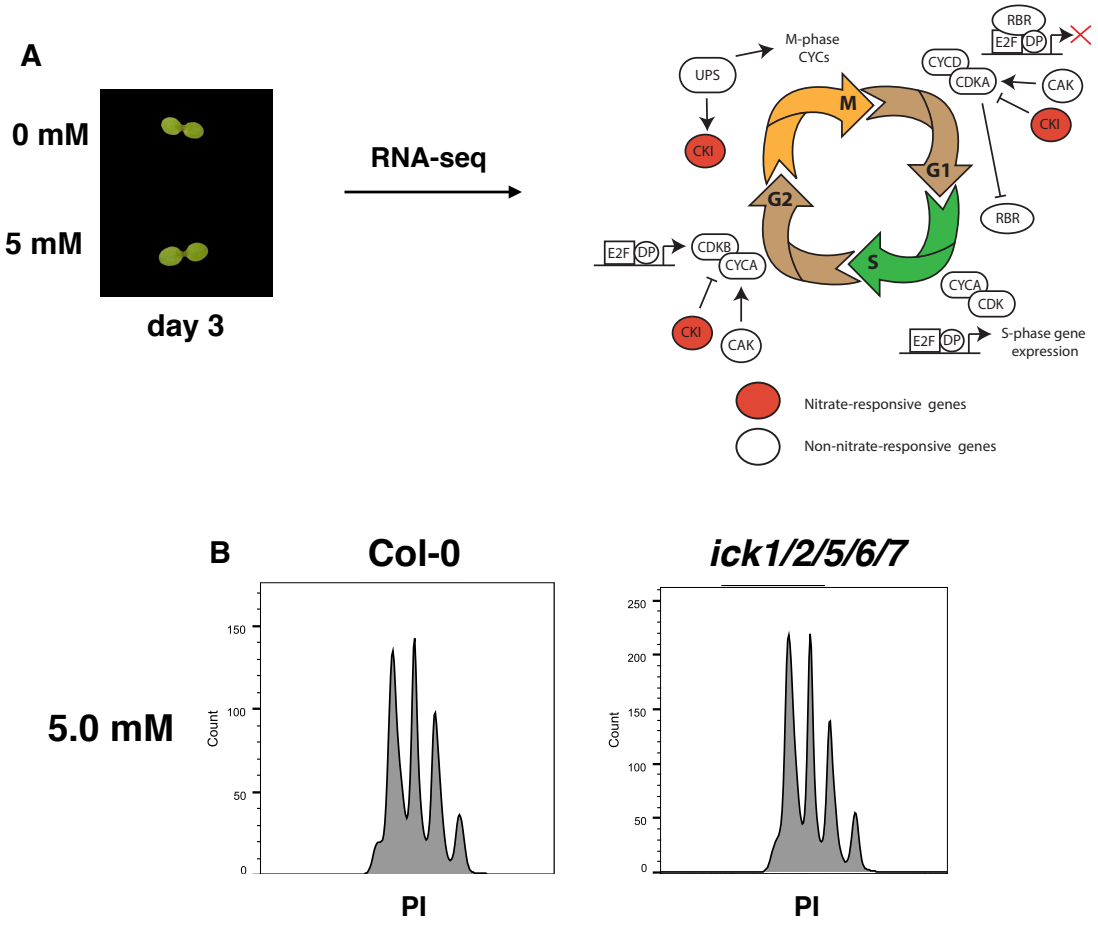

Figure 8 | Other cell cycle genes are not regulated by nitrate.
(A) Nitrate-responsive genes were analysis by RNA-seq from shoots of plants grown in two contrasting nitrate concentrations at 3 DAS. Cell-cycle genes differentially expressed in response to nitrate are represented by red circles in the scheme.
(B) Ploidy distribution of wild-type or *ick1/2/5/6/7* quintuple mutant. DNA content was measured by flow cytometry analysis. Plants were grown in 5 mM nitrate and cotyledons were chopped at 7 DAS

Nitrate regulates *LGO* expression on different cell-types.

In order to verify regulation of LGO expression under our experimental conditions as well as to gain insight into LGO's cell-type specific pattern of expression, we used the transcriptional reporter *pLGO::3XVENUS-N7 (*pDR67). As shown in Figure 9, the number of cells expressing the transcriptional reporter was significantly higher in cotyledons from plants grown in the presence of 5 mM nitrate as the only nitrogen source (Figures 9A-9E). Interestingly, while no differences were observed in both cell or cotyledon area by 3 DAS, many more cells expressed *LGO* under 5 mM as compared to 0 mM nitrate conditions. We also observed up-regulation of *LGO* in internal cells only in the presence of nitrate, consistent with our observation that ploidy is also increased in vegetative internal cell-layers by nitrate (Figure 9F and 9G).

These results indicate nitrate up-regulates expression of the key cell cycle regulatory gene *LGO*. Our data also indicates a pattern of LGO expression that is consistent with increased ploidy levels in response to increased nitrate supply. These results suggest LGO specifically mediates the increase in endoreplication which correlates with cell expansion as a result of increased nitrate supply.

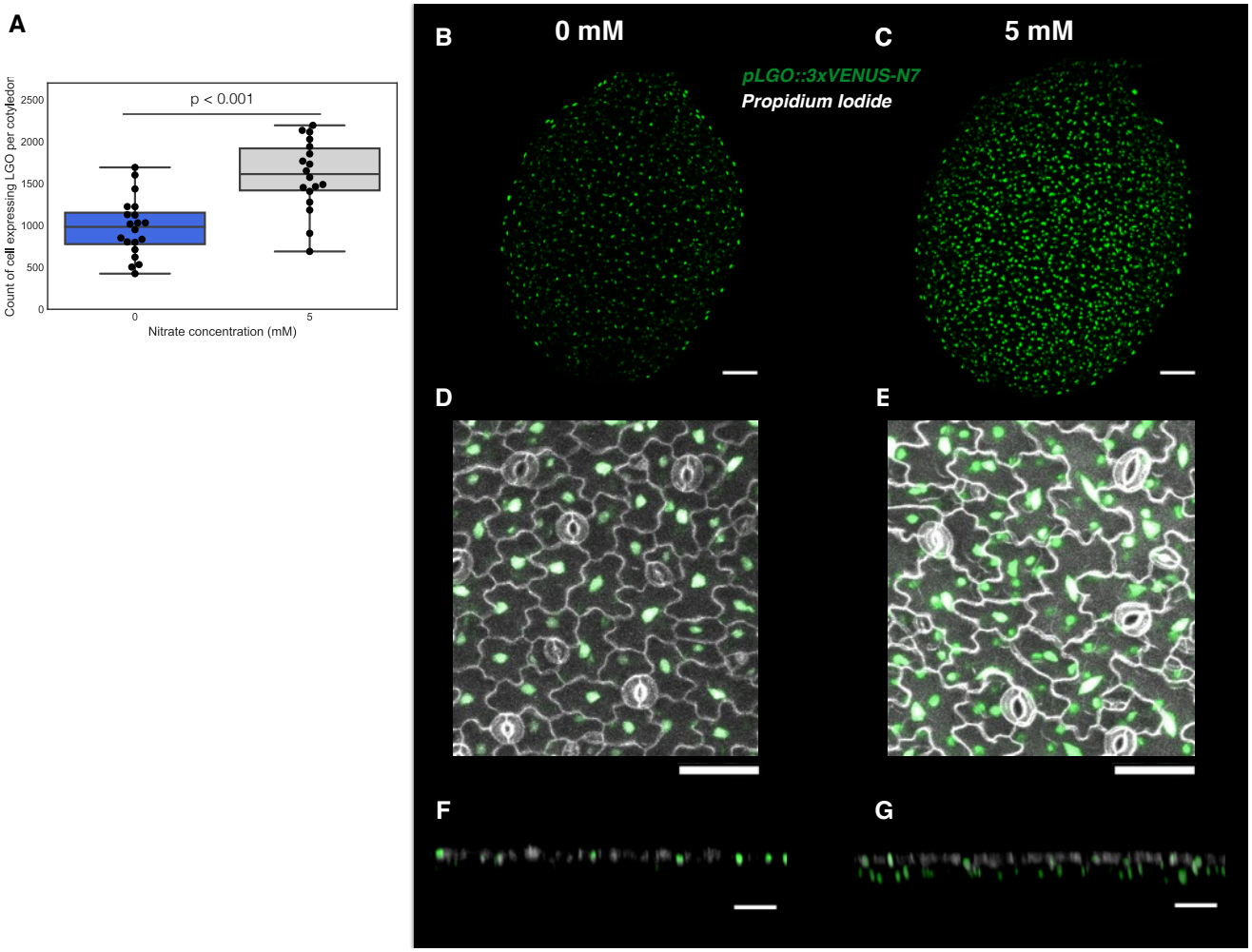

Figure 9 | Nitrate regulates *LGO* expression in different cell-types of Arabidopsis cotyledons.
(A) Count of cells expressing the transcriptional reporter *pLGO::3xVENUS-N7* in each cotyledon. Significant difference was detected by t-test analysis. Number of cells expressing fluorescent marker for each cotyledon were identified by CONSTANZA software.
(B-C) Representative cotyledon from transcriptional reporter lines *pLGO::3xVENUS-N7* (green) grown in 0 or 5 mM nitrate 3 DAS. Scale bars, 100 µm.
(D-E) Representative cotyledons from transcriptional reporter lines *pLGO::3xVENUS-N7* (green) grown in 0 or 5 mM nitrate 3 DAS. Plants were stained with PI (white) to label epidermal plasma membranes. Fluorescent nuclei indicate LGO expression. Scale bars, 100 µm.
(F-G) Representative images of transversal section of cotyledons stained with PI to mark epidermal cells. Fluorescent nuclei indicate LGO expression. Note that in 5mM nitrate, cells under the epidermis express *pLGO::3xVENUS-N7*, whereas in 0mM nitrate only epidermal cells express *pLGO::3xVENUS-N7.* Scale bars, 50 µm

LGO is required for nitrate-dependent endoreplication.

LGO is required for endoreplication in sepals and leaves (Roeder et al., 2010; Robinson et al., 2018). However, its role in response to nutritional status has never been assessed. First, we asked whether cell area induced by nitrate requires *LGO* function. We measured epidermal cell area of cotyledon cells in *lgo-2*, LGO-OX and WT plants grown under 0, 0.5 or 5 mM nitrate concentrations. We used the *ML1:LGO* as over-expression line of LGO (Robinson et al., 2018). Epidermal cells were stained with PI and cell area was quantified with MorphographX software at 7 DAS. In contrast to wild-type plants, where cell area increased from 3436.09 μm^2 to 4991.07 μm^2 when comparing 0.5 and 5 mM nitrate, epidermal cell area in *lgo-2* mutant plants barely increased with increased external nitrate concentration. We observed average epidermal cell area was 1911.65 μm^2 under 0.5 mM nitrate and 2069.89 μm^2 under 5 mM nitrate in *lgo-2* mutant plants (Figure 10A). On the contrary, we observed an increment in average epidermal cell area from 3514.48 to 6790.83 μm^2 in the LGO-OX line grown under 0.5 and 5mM, respectively.

Then, we asked whether LGO is required for nitrate-mediated endoreplication. A flow cytometry analysis was conducted in WT, *lgo-2* and LGO-OX plants grown under 0, 0.5 or 5 mM nitrate concentration. While cotyledon cells from *lgo-2* mutant plants revealed a significant enrichment of lower-order C values as compared to WT plant 7 DAS, over-expression of LGO showed higher-order ploidy profiles from plants grown under 5 mM nitrate (Figure 10B). We did not observe significant differences in ploidy profiles when comparing cotyledon cells from *lgo-2* mutant, LGO-OX and WT plants grown without nitrate (Figure 10C). However, *lgo-2* mutant cells showed significant differences in DNA content as compared to cells from wild-type when plants were grown with 5 mM nitrate (Figure 10B). For instance, an average of 40.8% and 24.6 % of 8C nuclei were observed in WT and *lgo-2* plants respectively in the presence of nitrate. 16C

nuclei were not observed in *lgo-2* plants under any nitrate condition. Interestingly, cotyledon cells in *lgo-2* mutant plants show endoreplication 3 DAS, suggesting an LGO-independent endoreplication process previous to the nitrate control of shoot growth: 8.5% of cells are 8C at day three in *lgo-2* mutant plants grown at 0, 0.5 or 5 mM nitrate(Figure 11A-C).

To confirm the specificity of LGO as a nitrate-required element for endoreplication, DNA content was measured in cotyledons of the mutant for another CKI mutant, *ick1/2/5/6/7* quintuple mutant plants (Figure 8B). Although this mutant has disrupted ploidy distribution in leaves (Cheng et al., 2015), we did not observe changes in the cotyledon DNA content in mutant as compared to wild-type plants under 5 mM nitrate regime, suggesting a specificity of LGO for endoreplication during nitrate-mediated growth.

Because we also observed nitrate-elicited higher ploidy levels in true leaves, we asked whether nitrate-mediated endoreplication in leaves also requires LGO. Flow cytometry analysis was conducted in the first pair of true leaves from plants grown under 0.5 or 5 mM nitrate concentrations. Significantly lower ploidy profiles were observed in *lgo-2* mutant plants grown under 5 mM as compared to wild-type plants (Figure 10C). These results indicate LGO plays a role in nitrate-elicited endoreplication in different shoot organs and developmental stages.

Finally, we inquired more in the role of LGO into the interplay between cell size and ploidy level. Because we can not identify the exact ploidy from confocal images, we used nuclei area as a proxy to identify the endoreplication level for each epidermal cells (Jovtchev et al., 2006). Wild-type and *lgo-2* plants were used as background for the double reporter lines pAR169/229 (*pATML1:: mCitrine-RCI2A* and *pATML1::H2B-mTFP*). Then, cell area and nuclei area were quantified from the same spot of epidermal cells in both genotypes. As we can see in Figure 10D, the correlation between nuclei and cell area is much lower in the *lgo-2* mutant compared to wild-

type. While cell size is mostly explained by endoreplication in wild-type plants ($r^2 = 0.9$, $p = 4.5e-46$), a lower correlation was observed in *lgo-2* mutant plants ($r^2 = 0.44$, $p = 2.2e-9$). As above-ground organ size is mainly explained by pavement cells, stomata cell lineages were excluded from the analysis.

Our results indicate LGO is necessary for nitrate-mediated endoreplication during cotyledon and leaf growth. Moreover, we observed that nitrate-elicited epidermal cell expansion is mainly triggered by LGO during shoot development.

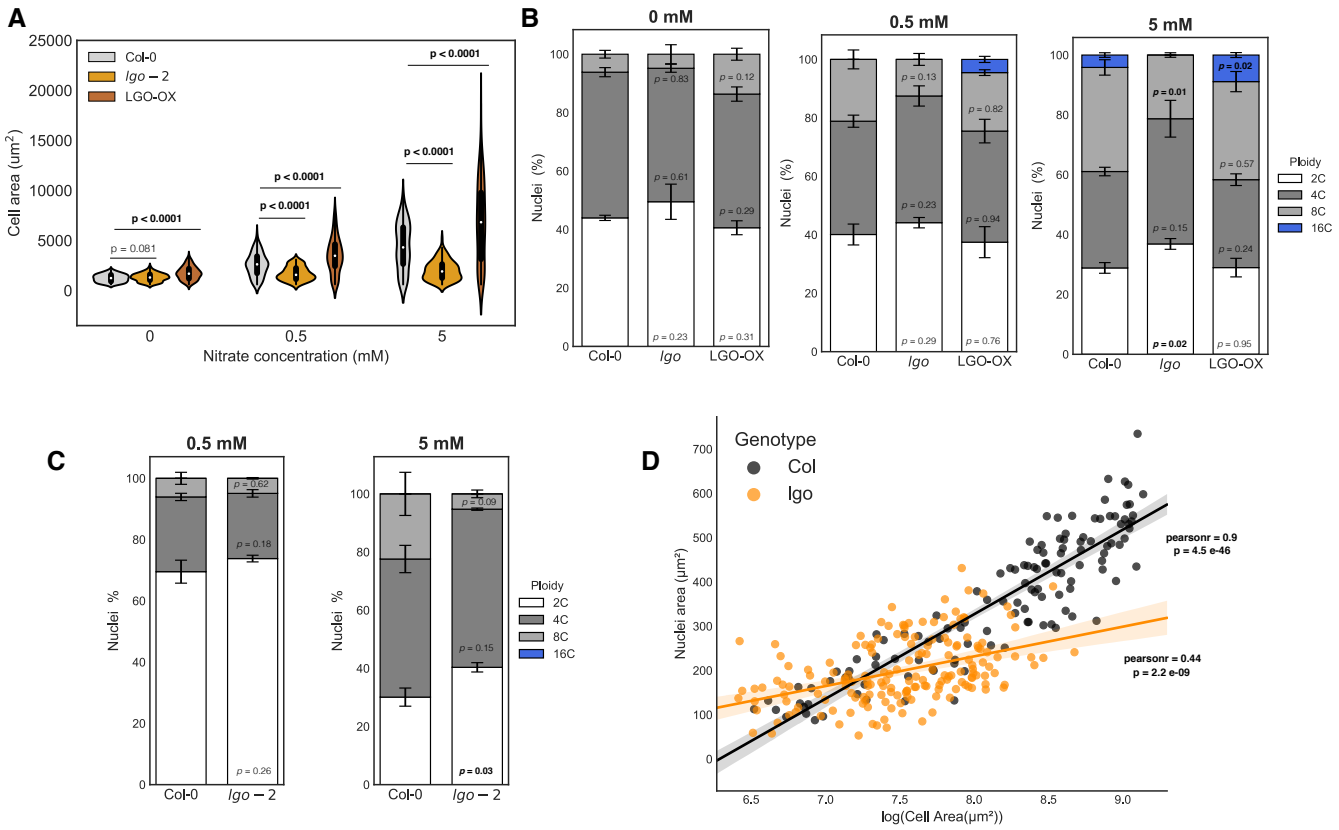

Figure 10 | Nitrate-promotes endoreplication through the CDK inhibitor LGO.
(A) Violin-plot representing epidermal cell area in wild-type, *lgo-2* and LGO-OX plants 7 DAS. Plants were grown in three nitrate conditions as mentioned before. Epidermal cells were stained with PI and cell area was measured using MorphographX software. White dots indicate median values. The ends of the black boxes are the upper and lower quartiles. Significant differences were detected by t-test analysis.
(B) Ploidy distribution analysis in cotyledons from wild-type, *lgo-2* and LGO-OX plants grown in three different nitrate concentrations 7 DAS (0, 0.5 or 5 mM Nitrate).
(C) Ploidy distribution in the first pair of true leaves from wild-type or *lgo-2* plants grown in 0.5 or 5 mM nitrate 15 DAS.
(D) Boxplot representing correlation between ploidy level (nuclei area) and cell area from wild-type and lgo-2 epidermal cells. Pearson correlation coefficient was used to quantified linear correlation between two variables.

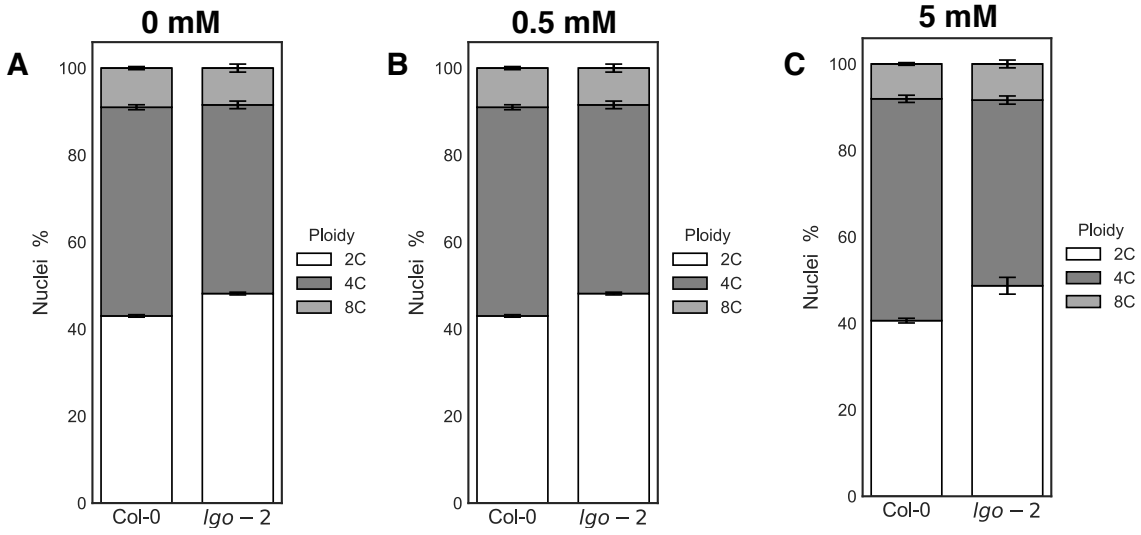

Figure 11 | Nitrate-promoted endoreplication through the CDK inhibitor LGO is not altered at 3 DAS.
(A) Flow cytometry analysis of DNA content in cotyledons from wild-type or *lgo-2* plants grown in 0 mM nitrate at 3 DAS.
(B) Flow cytometry analysis of DNA content in cotyledons from wild-type or *lgo-2* plants grown in 0.5 mM nitrate at 3 DAS.
(C) Flow cytometry analysis of DNA content in cotyledons from wild-type or *lgo-2* plants grown in 5 mM nitrate at 3 DAS.

Cell division compensates endoreplication to maintain nitrate-determined organ size.

Nitrate regulates spatial gene expression of *LGO* with consequences in ploidy profile and cell area. Because organ size is the product of cell area and cell number, we asked whether reduction or increment in cell area have consequences for organ size. Surprisingly, cotyledon organ size was not significantly different either in *lgo-2* or LGO-OX as compared to wild-type plants under 0, 0.5 or 5 mM nitrate concentrations (Figures 12A and 12B).

To better understand how nitrate determines organ size even when endoreplication is disrupted, we performed live-imaging analysis of *lgo-2* mutant cotyledons across the same time-course and nitrate concentrations described above for wild-type plants. Cells were segmented using MorphographX software and each cell lineage was labeled to evaluate cell proliferation and cell expansion. The double marker line pAR169/229 was used in the *lgo-2* mutant plants to mark plasma membranes and nuclei (*pATML1:: mCitrine-RCI2A* and *pATML1::H2B-mTFP*) (Figures 12C and 12E). Stomatal cell lineages were excluded from our cell tracking analysis as mentioned above. Pavement cells divided over time in cotyledons of *lgo-2* mutant as compared to those from wild-type plants where we observed no cell division (Figures 12D and 12F in comparison with 4A and 4B; 273 and 206 cell pavement lineages were tracked in *lgo-2* mutant plants grown under 0 or 5 mM nitrate respectively). At the end of the time-course, 28 % of *lgo-2* pavement cell lineages have gone through at least one round of cell division in plants grown under 5 mM nitrate (Figure 12F). In contrast, none of the pavement cell lineages in *lgo-2* plants have gone through a round of cell division when grown under 0 mM nitrate from 3 to 7 DAS (Figure 12D).

We then asked whether cell expansion and cell proliferation were collectively acting to increase organ size in the presence of nitrate in *lgo-2* mutant plants. Cumulative cell growth was measured for each cell lineage from *lgo-2* mutant plants during the five-day time-course (Figure

13A-13C). We define a cell lineage as all the cells descended from a single cell in the first time point 3 DAS. Thus, one cell lineage in *lgo-2* plants is equivalent to one undivided cell in wild-type plants. Similar to wild-type, cell lineage growth was increased in the presence of nitrate. Whereas cell lineage expanded an average of 1.89 times in plants grown under 0 mM nitrate, cell lineages expanded an average of 3.87 times in *lgo-2* mutant plants grown under 5 mM. These rates are similar to those observed in wild-type plants.

We then asked why some pavement cells in *lgo-2* plant cotyledons went through one round of cell division (~30% of the cell lineages) while others did not (Figure 12G). To gain insight into the mechanism behind cell size control of LGO, we separated proliferated and non-proliferated epidermal cell lineages from *lgo-2* plants grown under 5 mM nitrate for each day. Once a cell lineage has proliferated, it was not considered for analysis in next days. Interestingly, we observed that proliferated cell lineages are significantly bigger than non-proliferated cells in *lgo-2* plants after 5 DAS. In addition, differences in lineage cell area increased over time (Figure 12H). Our results are consistent with a coupling of cell size with the cell division, which has been observed previously in the meristem (Jones et al., 2017).

Our results indicate LGO acts as a cell cycle control factor that integrates external nitrate signal to promote endoreplication. Interestingly, under our experimental conditions cell proliferation can compensate for endoreduplication to reach a specific organ size defined by external nitrate availability. This result suggests nitrate interacts with an organ-level control mechanism to define organ size.

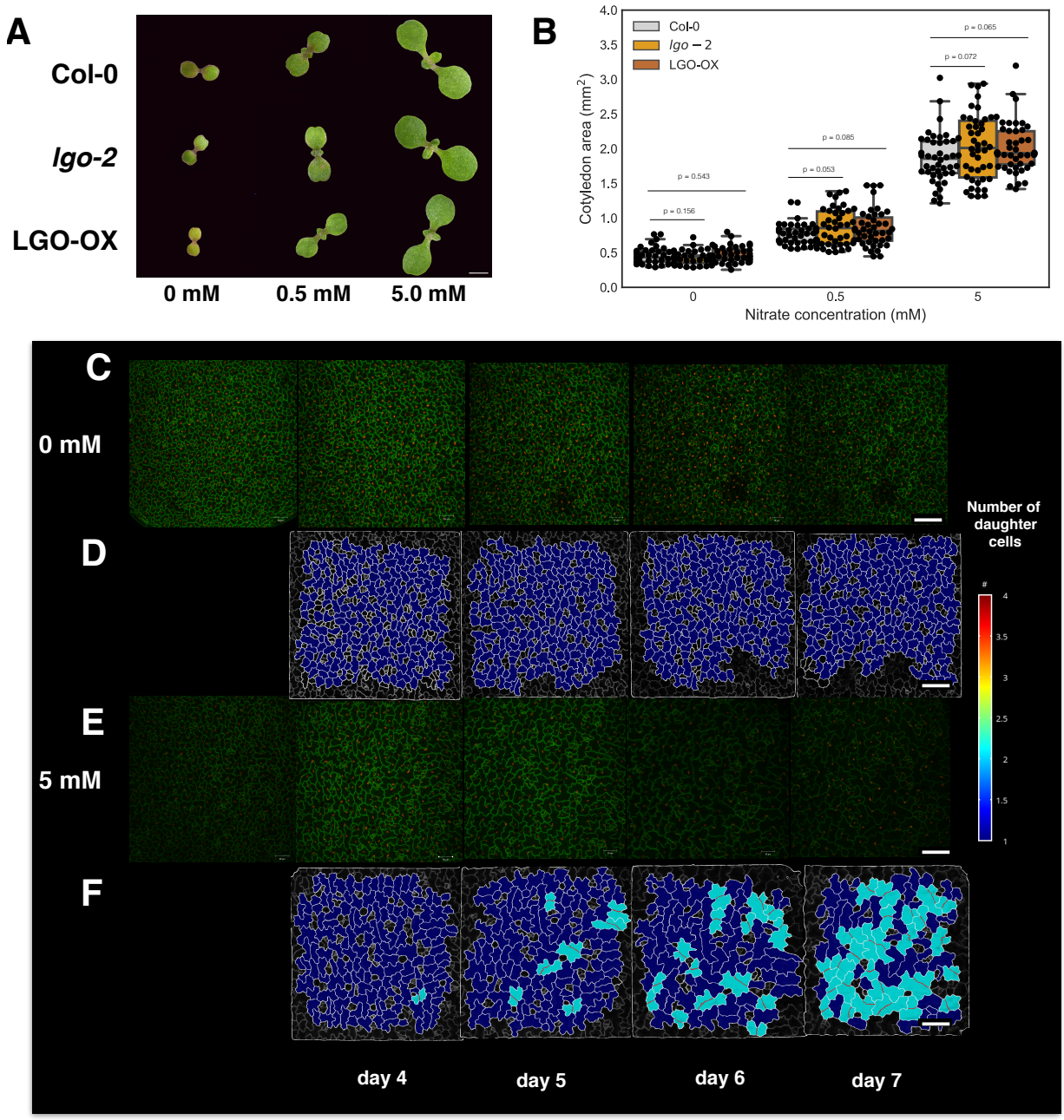
A
Col-0
lgo-2
LGO-OX
0 mM
0.5 mM
5.0 mM
B
Col-0
lgo – 2
LGO-OX
Cotyledon area (mm²)
Nitrate concentration (mM)
p = 0.543
p = 0.156
p = 0.085
p = 0.053
p = 0.065
p = 0.072
C
0 mM
D
E
5 mM
F
Number of daughter cells
day 4
day 5
day 6
day 7
G
Percentage of cells having divided (%)
Days
H
Proliferated
Non proliferated
Lineage cell area (µm²)
Day
p = 0.245
p = 0.002
p < 0.001
p < 0.001

Figure 12 | Organ size compensation process in response to nitrate status.
(A) Representative figure of wild-type, *lgo-2* and LGO-OX seedlings grown in three different nitrate concentrations (0, 0.5 or 5 mM). Scale bars, 1 mm.
(B) Quantification of cotyledon size in wild-type, *lgo-2* and LGO-OX plants grown in three different nitrate concentrations 7 DAS. n = 30 seedlings for each point, three independent replicates. Cotyledon size were compared using t-test for each nitrate concentration
(C and E) Confocal stack maximum-intensity projections of cotyledons from *lgo-2* mutant cotyledons grown in two contrasting nitrate concentrations (0 or 5 mM). Epidermal cells were labeled in green with the reporter *pATML::mCitrine-RCl2A*. Nuclei were labeled in red with reporter *pATML1::H2B-mTFP*. Epidermal cells of cotyledons were imaged every 24 horas from 3 to 7 DAS.
(D and F) Heatmaps of cell division rate in *lgo-2* cotyledons of plants grown in 0 mM or 5 mM nitrate. Cell division rate was calculated relative to day 3. Every new cell wall was labeled by a red line. Epidermal cell area from *lgo-2* mutant plants were segmented and analyzed with MorphographX.
(G) Bar plot showing percentage of proliferated pavement cell lineages in response to nitrate (5 mM). Percentage is the representation of three biological replicates.
(H) Boxplot showing cell area average of proliferated and non-proliferated of pavement cell lineages from *lgo-2* mutant plants from day 4 to 7 DAS. Once cell lineage has proliferated, it was not considered for next days. White dots indicate median values. The ends of the black boxes are the upper and lower quartiles. Significant difference was detected by t-test analysis using same sample size for each statistics analysis. Scale bars, 100 µm.

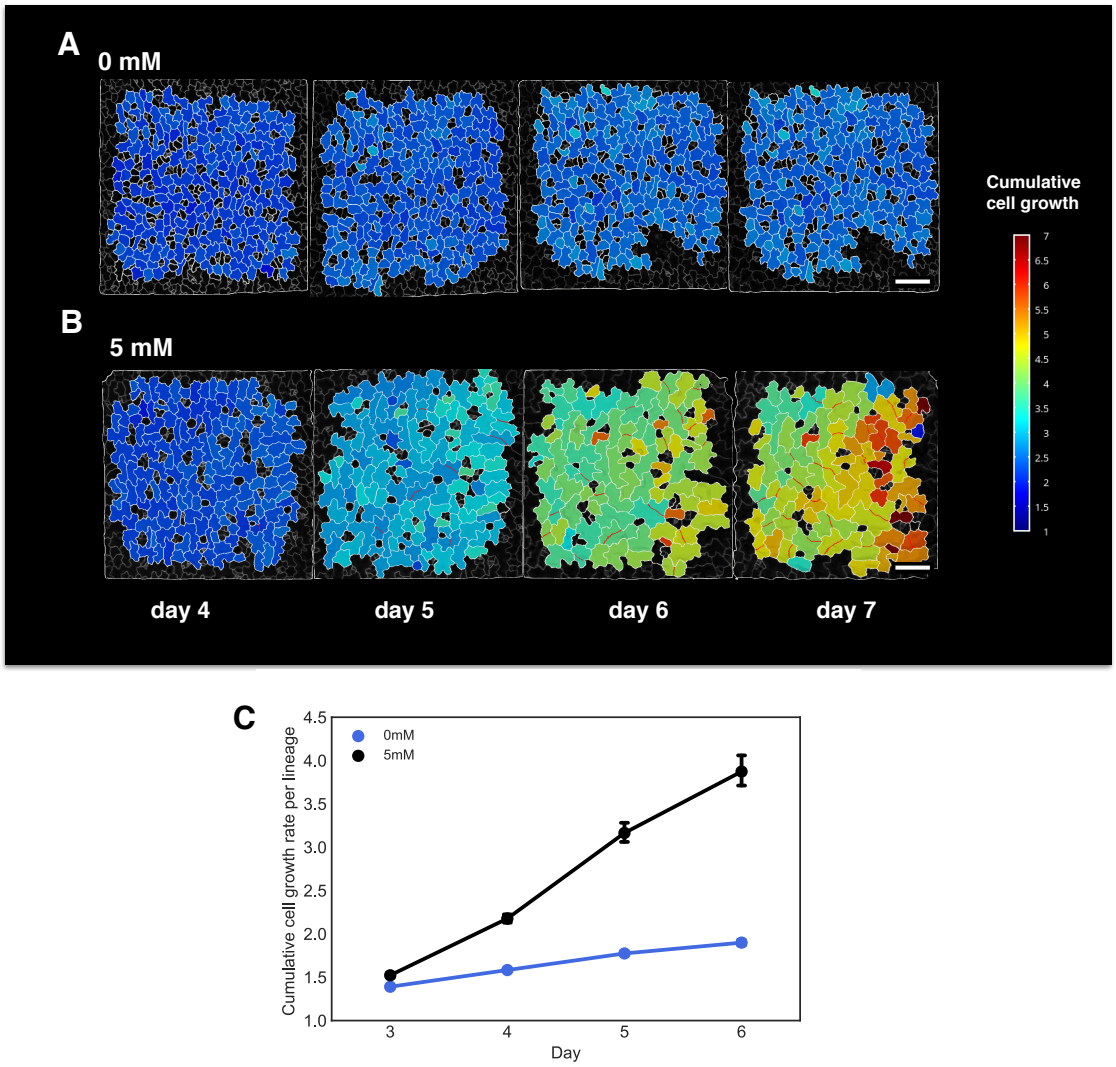

Figure 13 | Nitrate-determined organ size is attained by cell division and cell expansion in *lgo-2*.

(A and B) Heatmap of cumulative cell growth of *lgo-2* cotyledon cell lineages. Confocal stack maximum-intensity projection images were obtained from plants grown in two different nitrate concentrations (0 mM or 5 mM). Epidermal cells were segmented and tracked with MorphographX software.

(C) Cumulative cell growth average for each cell lineage. Cumulative cell growth was calculated using the same cell lineages in Figure 12G.

AIM 3

In order to decode the regulatory elements that act up-stream of *LGO* in the nitrate-mediated shoot growth described above, we added new information to the transcriptional data obtained by RNA-seq previously mentioned. A recent proliferation of Transcription Factor (TF) - target binding data has emerged from high-throughput *in vitro* approaches such as DNA affinity purification sequencing (DAP-seq) (O'Malley et al., 2016). DAP-seq is a technique that couples affinity-purified TFs with next-generation sequencing of a genomic DNA library. O'Malley and collaborators described the *Arabidopsis* cistrome by resolving motifs and peaks for 529 TFs from *Arabidopsis thaliana* genome.

We assessed whether some of the differentially expressed genes in response to nitrate bind to LGO promoter in DAP-seq data. We identified 119 TF that interacts with the LGO promoter in DAP-seq data. Interestingly, six of them were also regulated at transcriptional level by nitrate 3 DAS: *NAP*, *SVP*, *GATA4*, *AT5G25810*, *HAT2* and *TGA1*. Moreover, TGA1 and NAP have been previously described as part of nitrate signaling pathway (Alvarez et al., 2014). We asked whether TGA1 or NAP regulate some of nitrate-mediated effects on shoot growth described in this study.

First, we conducted an analysis in the double mutant *tga1*/*tga4.* We used the double mutant because reported functional redundancy between TGA1 and TGA4 transcription factors. As we can see in Figure 14A, shoot area was similar between wild-type and mutant plants for all nitrate concentrations. As we observed in *lgo-2* mutant plants, cell expansion can be substituted by cell proliferation to reach same organ size. Therefore, we asked whether we could see the same phenomenon in the double mutant *tga1/tga4*. We quantified ploidy profiles by flow cytometry approach from plants grown under different concentration of nitrate 7 DAS. However, as we can

observed in Figure 14B, ploidy profiles were similar in double mutant *tga1/tga4* and wild-type cotyledons. Actually, we can observe a slight increment of higher ploidy levels in mutant plant grown under 5 mM nitrate. Thus, we concluded that TGA1 and TGA4 seems to be irrelevant in the nitrate-mediated post-embryonic growth.

Since the availability to bind a promoter *in vitro* does not mean that a transcription factor is really regulating that specific gene *in vivo*, we needed another approach to decode the transcription factor that regulates LGO in response to nitrate during this developmental stage. We concluded from *tga1/tga4* results that DAP-seq analysis were not enough to decode TF regulating LGO at this developmental stage. Although TGA1 was observed bound to the LGO promoter, phenotypes described in Figure 14 show that TGA1 is not responsible for LGO role during nitrate-mediated shoot growth.

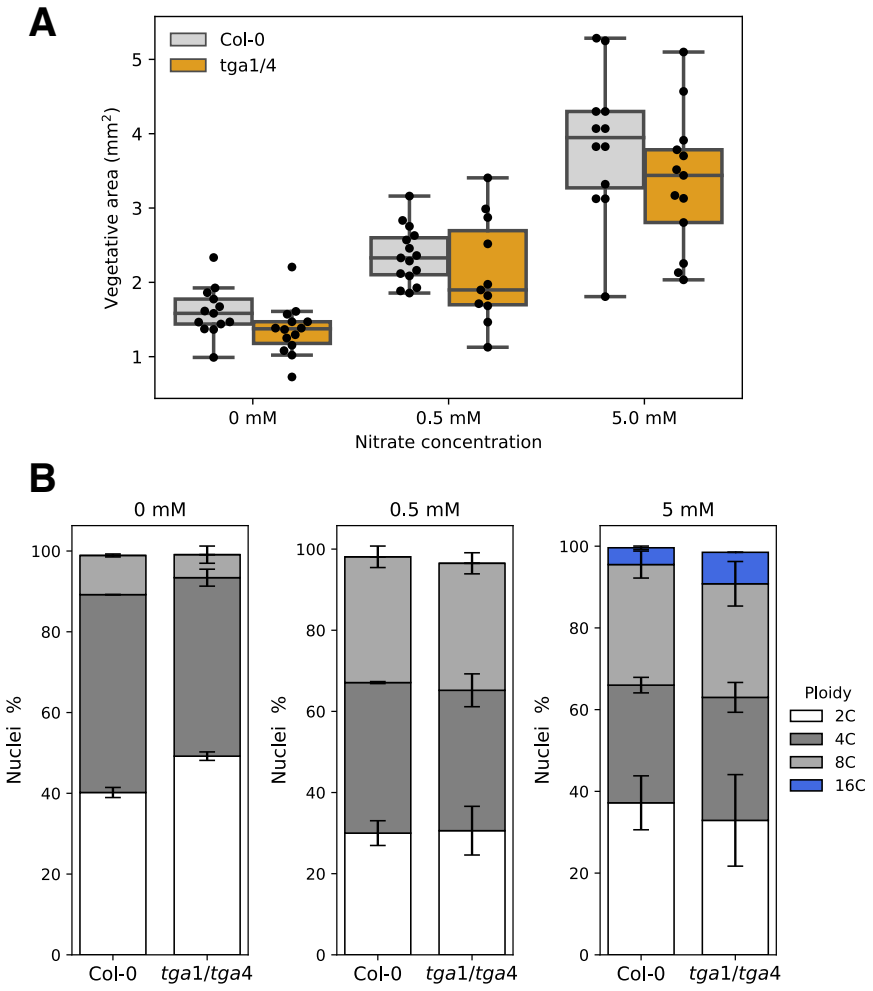

Figure 14 | Nitrate-mediated post-embryonic growth is not regulated by TGA1 or TGA4.
(A) Plants were grown under different nitrate concentrations (0 mM, 0.5 mM and 5.0 mM) and photographed 7 DAS.
(B) Ploidy distribution in cotyledons from wild-type or *tga1/tga4* plants grown in 0, 0.5 and 5 mM nitrate 7 DAS.

Another alternative to identify up stream transcription factors is to analyze transcriptional correlations between TF and target. In order to see whether some of the transcription factors identified by DAP-seq also correlates with LGO expression at transcriptional level, we conducted a co-expression transcriptional network with published and unpublished RNA-seq libraries. We used 70 RNA-seq libraries from plants that were treated with different concentrations of nitrate at different time-points. Since our work has focused only in above-ground organs, we used only libraries from shoot tissues to perform the co-expression network. Then, we filtered TF-target interactions to include pairs for which expression values are highly and significantly correlated (pearson correlation coefficient >0.8).

As we can see in Figure 15, our analysis identified one transcription factor co-expressed with the cell cycle gene LGO: HAT2. The gene encoding transcription factor HAT2 has been described as auxin-inducible, this TF plays opposite roles in shoot and root tissue regulating auxin-dependent morphogenesis. Recently, this transcription factor has been related to leaf development and pavement cell differentiation(Challa et al., 2019). Thus, HAT2 seems a good candidate to explain part of nitrate-mediated shoot growth. The next step will be to confirm whether HAT2 binds to LGO in our experimental approach and whether this transcription factor has a relevant impact during nitrate-mediated shoot growth described in this work.

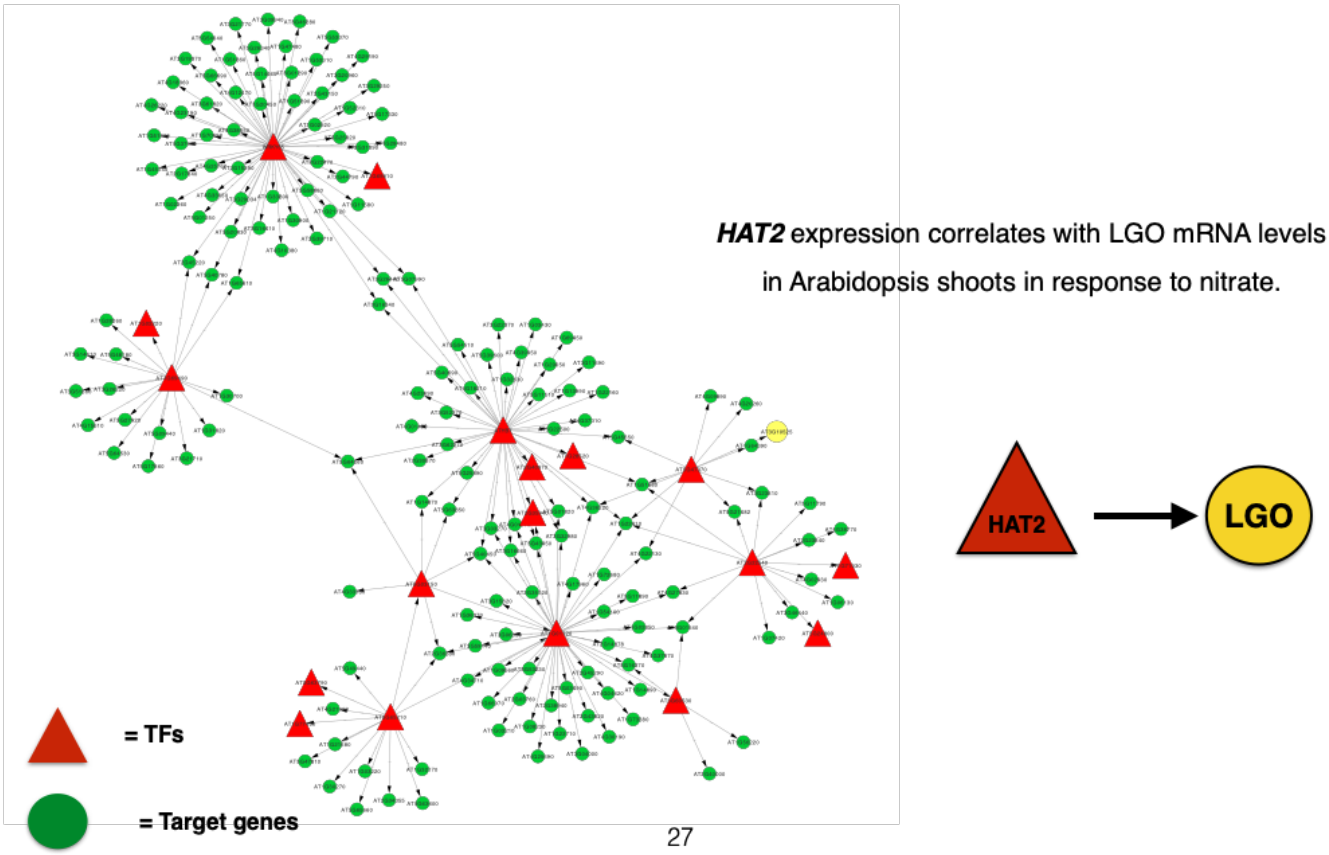

Figure 15 Co-expression network analysis from transcriptomics data. Transcriptional factors are drawn as red triangles and putative targets are drawn as green circles. Black lines indicate predicted transcriptional activation according to DAP-seq approach (O'Malley et al., 2016). LGO is represented as a yellow circle.

DISCUSSION

We aimed to understand molecular mechanisms underlying nitrate-mediated shoot growth. We found that nitrate coordinates cell expansion and endoreplication by regulating the expression of *LGO*, a plant-specific cell cycle inhibitor. We showed that organ size is determined by N-nutritional status even in the absence of LGO-mediated endoreplication. Our results indicate that nitrate has an important role in defining shoot organ size during Arabidopsis development.

Nitrate mediates post-embryonic growth by cell expansion.

Several studies reported that shoot growth is regulated by nitrate availability (Liu et al., 2017; Poitout et al., 2018). Our data are consistent with these early results, supporting a specific role of nitrate in control of post-embryonic shoot growth. We showed external nitrate is sensed by the plant shortly after germination and modulates cotyledon growth as early as 4 DAS. Our results indicate NRT1.1 and NLP7, important components in the nitrate signaling pathway, are required for normal nitrate-induced post-embryonic growth (Figure 1D and 1E). Interestingly, we observed that *chl1-5* mutant plants, which lack a functional NRT1.1 transceptor, were smaller than wild-type even in the absence of nitrate. Our results are consistent with a previous study that mentioned the role of the transporter NRT1.1 during embryonic developmental stages, explaining why *chl1-5* are smaller regardless the environmental concentration of nitrate (Alboresi et al., 2005). We observed lower-order level ploidy in *chl1-5* and *nlp7-1* mutant as compared to wild-type plants under sufficient nitrate conditions. TGA1/TGA4 have been described as master transcription factors commanding nitrate response in Arabidopsis roots (Alvarez et al., 2014). We used the

tga1/tga4 double mutant line to test whether these transcription factors were involved in this process. However, no differences in ploidy levels were observed between double mutant and wild-type plants (data not shown). Since endoreplication and plant growth still occurs in both *chl1-5* and *nlp7-1* mutant lines, additional regulatory elements or nitrate-signaling components may be involved in this process. It can be explained because most regulatory elements within nitrate signaling pathway, such as NRT1.1 and NLP7, have been described in roots. However, recent publications have identified regulatory elements commanding nitrate signaling in shoots (Varala et al., 2018; Brooks et al., 2019). To evaluate whether some of these new elements regulate nitrate-mediated endoreplication and cell expansion is the next step forward.

Post-embryonic cellular dynamics of plant cotyledons have been controversial. While some studies argue that cell proliferation occurs only during embryogenesis (Tsukaya et al., 1994; Armour et al., 2015), others studies have described some degree of cell proliferation in light-grown cotyledons (Fridlender et al., 1996; Stoynova-Bakalova et al., 2004). Our cotyledon live-imaging experiments provided an unprecedented level of detail monitoring post-embryonic epidermal cellular dynamics from plants grown under different nitrate conditions. Under our experimental conditions, cell proliferation was only observed in cells from stomatal lineage (data not shown), which indicates that cell division is not relevant for vegetative area growth in cotyledons of wild-type Arabidopsis early after germination.

Cell behavior is highly heterogeneous (Hong et al., 2018). How organisms coordinate cellular heterogeneity to achieve robustness at organismal scales has been largely unknown (Serrano-Mislata et al., 2015; Long and Boudaoud, 2019). Above-ground tissues are characterized by high levels of heterogeneity in cell size, which in turn is explained by heterogeneity in cell cycle and cell wall stiffness (Cosgrove, 2018; Eng and Sampathkumar, 2018; Hong et al., 2018).

Through our cotyledon live-imaging approach, we show nitrate triggers a switch in epidermal cotyledon cell size from a homogeneous to a heterogeneous state (Figure 3). Finally, our results re-define cotyledons as a useful model system for a better understanding of developmental processes such as cell expansion and endoreplication and their coordination to achieve proper organ size.

Nitrate-elicited endoreplication by LGO.

The absence of correlations in some experiments between cell growth and endoreplication have raised questions about the physiological significance and the role of endoreplication (Sliwinska et al., 2009; Lee et al., 2010). Some studies associated endoreplication to environmental stress signals such as light (Gegas et al., 2014), drought (Dubois et al., 2013), salt (Ceccarelli et al., 2006), pathogens (Bainard et al., 2011), among others. Indeed, endoreplication has been proposed as a generalized stress response in plants (Scholes and Paige, 2015). Moreover, endoreplication is usually confined to specialized cell types with specific biological functions (Lee et al., 2010). Our results support endoreplication as a basic mechanism to promote and control shoot organ growth and size. The clear correlation between nuclei area and cell area in wild-type plants support the idea of a causal-effect connection between cell expansion and endoreplication (Figure 10D). However, the absence of experiments in our work that directly correlates ploidy level (2C, 4C, etc) with cell size over time prevents us to conclude that cell expansion in pavement cells is solely explained by endoreplication.

Our results also showed that nitrate promoted higher-order ploidy levels in cotyledon and leaves largely via LGO, a cell cycle inhibitor that has been previously connected to ploidy and cell size control mainly in sepals (Roeder et al., 2010). Ploidy levels were significantly lower in *lgo-2* mutant compared to wild-type plants both in cotyledon and leaves. In addition, correlation

between nuclei and cell area was much lower in mutant plants compared to wild-type. We can conclude that part of the causal-effect relationship between endoreplication and ploidy level observed in wild-type is explained by LGO. However, cell expansion observed from some lineages in *lgo-2* mutant plants (Figure 12H and 13C), slight increment of ploidy level in the absence of LGO (Figure 10B), and the still presence of correlation between nuclei area and cell size in *lgo-2* mutant plants, support the idea that LGO is only partially responsible for the nitrate-mediated cell expansion process and it seems to have a dual role on endoreplication and cell expansion.

Some minor discrepancies between our results and previous works can be attributed to the developmental stage or tissues used in flow cytometry analysis. For instance, Hamdoun's work (2016) conducted a flow cytometry analysis from 4^{th}-6^{th} leaves at 25 DAS. On the other hand, our flow cytometry analysis from leaves was conducted 15 DAS from the first-pair of true leaves. Despite this minor discrepancies, our results with LGO-null lines are consistent with Hamdoun's and other reports (Roeder et al., 2010; Hamdoun et al., 2016; Robinson et al., 2018).

LGO was previously reported as a nitrate-responsive gene in shoots (Varala et al., 2018). However, its role had not previously been assessed in response to the plant nutritional status. Only a handful of studies addressed the mechanism underlying the interaction between cell cycle progression and plant growth in response to nitrate, all of them in the nitrate control of root growth. For instance, the nitrate-responsive transcription factors TCP20, NLP6 and NLP7 modulate expression of cell-cycle progression gene *CYCB1;1*, controlling cell division in the root meristem in response to nitrate starvation (Guan et al., 2017). Our findings regarding nitrate-triggered endoreplication mediated by LGO regulation is a step forward towards understanding the interplay between cell-cycle and nitrate-responsive processes in shoots. Our results showed that vegetative cells endoreplicate at very early stages of development (3 DAS) in wild-type and *lgo-2* mutant

plants. Approximately 60% of epidermal and internal nuclei cells have gone through at least one round of DNA replication in both genotypes before 3 DAS. This result is consistent with prior reports that show endoreplication begins early after germination in cotyledon cells (Sliwinska et al., 2009).

Organ size is defined by nitrate status.

Our results show that plants integrate nitrate status to determine organ size. In wild-type plants, nitrate promotes cell expansion via endoreplication allowing organs to grow to specified sizes. Our transcriptomic studies show nitrate causes upregulation of *LGO* gene expression. Upregulation of LGO, promotes endoreplication and cell expansion for nitrate-induced cotyledon growth. Interestingly, our results also demonstrate that endoreplication *per se* is not required for organ growth to a nitrate-specified size. In the *lgo* mutant and LGO-OX line, where endoreplication is greatly reduced or highly increased, organ size is unaffected, and still specified by nitrate availability. Our live imaging demonstrates that cell lineage growth is equivalent in wild-type and *lgo* mutant plants (Figure 11 and 12). In *lgo* mutant plants, cells divide instead of endoreplicating and indicating that equivalent growth can be achieved by either mitotic cycles or endocycles. Compensation phenomenon has been mainly described as cell enlargement triggered by a significant decrease in cellular proliferation (Ferjani et al., 2007; Horiguchi and Tsukaya, 2011; Tsukaya, 2019). Our results are consistent with previously described compensatory processes. Nitrate seems to increase LGO-dependent cell expansion and mitosis. Then, in the absence of LGO, mitosis is enhanced as we can observe in Figure 12.

Organ size robustness has been reported in other tissues such as sepals and leaves from LGO-null mutant plants (Roeder et al., 2010; Robinson et al., 2018). Sepal area was substantially

identical in *lgo-2* mutant as compared to wild-type plants (Robinson et al., 2018). These analyses on LGO-null lines or LGO-OX lines were conducted under nutritionally sufficient conditions. We extend this result to show that organ size is robust to the loss of LGO under contrasting nitrate concentrations, with organs still attaining the correct size in response to external nitrate availability, regardless of major changes in cell-cycle control. Yet the mechanisms underlying organ size control are unknown in plants. This is certainly an exciting area for future efforts.

Besides epidermal cells, shoot size could be enhanced due to more cells initially recruited in shoot apical meristem (Gonzalez et al., 2012). *WUSHEL* (*WUS*) and cytokinin precursors (tZR) are up-regulated by nitrate, triggering an enhancement of meristem size and organogenesis rate (Landrein et al., 2018), suggesting that rosette enlargement by nitrate availability could be triggered somehow at a meristematic level. In addition to nitrate-elicited modulation of cytokinins and *WUS* at SAM level, our results add cell expansion as a new mechanism to achieve nitrate-defined organ size. Since post-embryonic growth of cotyledon is explained independently of shoot apical meristem, our results suggest that nitrate-mediated cell expansion probably occurs separately from SAM behavior in response to nitrate at least during early developmental stages. Whether the dynamics of SAM and epidermal cells are coordinated in response to nitrate supply in posterior developmental stages remains unknown.

Our results showing how nitrate impinges on the cell cycle increase our understanding behind a largely described but still unexplained nitrate control of vegetative area. Our results provide an entry point towards better understanding of the role of nitrate in controlling shoot size, which has not been explored thus far. Understanding above-ground plant size in response to N-availability is important for crop yield. Our work represents a first step towards developing biotechnological solutions to improve nitrogen use efficiency for sustainable agriculture.

CONCLUSIONS

- Nitrate signaling is important for shoot growth early after germination.
- Cell expansion plays an important role in nitrate-mediated cotyledon growth.
- Nitrate sensing promotes cell expansion through endoreplication.
- Nitrate regulates *LGO* expression on different cell-types.
- LGO is required for nitrate-dependent endoreplication.
- Cell division compensates endoreplication to maintain nitrate-determined organ size in the absence of LGO.

Supplementary Table 1. Cell cycle genes regulated in response to nitrate 3 DAS.

AGI	name	baseMean	log2Fold Change	lfcSE	stat	pvalue	padj
AT3G10525	**SIAMESE RELATED 1 (SMR1) (LGO)**	**114.592234 420883**	**0.73540921 9770873**	**0.188**	**3.908**	**9.29e-05**	**0.00108**
AT3G51280	Tetratricopeptide repeat (TPR)-like	91.4671140 087321	0.93341430 4464214	0.232	4.013	5.98e-05	0.00074
AT3G53230	CELL DIVISION CYCLE 48B	109.808666 725304	1.16255458 322748	0.198	5.855	4.74e-09	0.00000
AT5G51600	MICROTUBULE-ASSOCIATED PROTEIN 65-3	100.515436 209951	0.76669235 1818155	0.203	3.758	0.00010	0.00183

BIBLIOGRAPHY

Alboresi A, Gestin C, Leydecker MT, Bedu M, Meyer C, Truong HN (2005) Nitrate, a signal relieving seed dormancy in Arabidopsis. Plant, Cell Environ **28**: 500–512

Alvarez JM, Riveras E, Vidal EA, Gras DE, Contreras-López O, Tamayo KP, Aceituno F, Gómez I, Ruffel S, Lejay L, et al (2014) Systems approach identifies TGA1 and TGA4 transcription factors as important regulatory components of the nitrate response of Arabidopsis thaliana roots. Plant J **80**: 1–13

Andriankaja M, Dhondt S, DeBodt S, Vanhaeren H, Coppens F, DeMilde L, Mühlenbock P, Skirycz A, Gonzalez N, Beemster GTS, et al (2012) Exit from Proliferation during Leaf Development in Arabidopsis thaliana: A Not-So-Gradual Process. Dev Cell **22**: 64–78

Araus V, Vidal EA, Puelma T, Alamos S, Mieulet D, Guiderdoni E, Gutiérrez RA (2016) Members of BTB gene family regulate negatively nitrate uptake and nitrogen use efficiency in Arabidopsis thaliana and Oryza sativa. Plant Physiol **171**: pp.01731.2015

Armour WJ, Barton DA, Law AMK, Overall RL (2015) Differential Growth in Periclinal and Anticlinal Walls during Lobe Formation in Arabidopsis Cotyledon Pavement Cells. Plant Cell **27**: 2484–2500

Arumuganathan K, Earle ED (1991) Nuclear D N A Content of Some Important Plant Species. **9**: 208–218

Bainard LD, Bainard JD, Newmaster SG, Klironomos JN (2011) Mycorrhizal symbiosis stimulates endoreduplication in angiosperms. Plant, Cell Environ **34**: 1577–1585

Barbier de Reuille P, Routier-Kierzkowska AL, Kierzkowski D, Bassel GW, Schüpbach T, Tauriello G, Bajpai N, Strauss S, Weber A, Kiss A, et al (2015) MorphoGraphX: A

platform for quantifying morphogenesis in 4D. Elife **4**: 1–20

Beemster GTS, De Veylder L, Vercruysse S, West G, Rombaut D, Van Hummelen P, Galichet A, Gruissem W, Inzé D, Vuylsteke M (2005) Genome-wide analysis of gene expression profiles associated with cell cycle transitions in growing organs of Arabidopsis. Plant Physiol **138**: 734–743

Berckmans B, Lammens T, Van Den Daele H, Magyar Z, Bogre L, De Veylder L (2011) Light-Dependent Regulation of DEL1 Is Determined by the Antagonistic Action of E2Fb and E2Fc. Plant Physiol **157**: 1440–1451

Bergmann DC, Sack FD (2007) Stomatal Development. Annu Rev Plant Biol **58**: 163–181

Bramsiepe J, Wester K, Weinl C, Roodbarkelari F, Kasili R, Larkin JC, Hülskamp M, Schnittger A (2010) Endoreplication controls cell fate maintenance. PLoS Genet **6**: 1–14

Brooks MD, Cirrone J, Pasquino A V., Alvarez JM, Swift J, Mittal S, Juang CL, Varala K, Gutiérrez RA, Krouk G, et al (2019) Network Walking charts transcriptional dynamics of nitrogen signaling by integrating validated and predicted genome-wide interactions. Nat Commun **10**: 1–13

Canales J, Contreras-López O, Álvarez JM, Gutiérrez RA (2017) Nitrate induction of root hair density is mediated by TGA1/TGA4 and CPC transcription factors in Arabidopsis thaliana. Plant J **92**: 305–316

Cebolla A, Vinardell JM, Kiss E, Oláh B, Roudier F, Kondorosi A, Kondorosi E (1999) The mitotic inhibitor ccs52 is required for endoreduplication and ploidy-dependent cell enlargement in plants. EMBO J **18**: 4476–4484

Ceccarelli M, Santantonio E, Marmottini F, Amzallag GN, Cionini PG (2006) Chromosome endoreduplication as a factor of salt adaptation in Sorghum bicolor. Protoplasma **227**: 113–

118

Challa KR, Rath M, Nath U (2019) The CIN-TCP transcription factors promote commitment to differentiation in Arabidopsis leaf pavement cells via both auxin-dependent and independent pathways. PLoS Genet **15**: 1–30

Cheng Y, Liu H, Cao L, Wang S, Li Y, Zhang Y, Jiang W, Zhou Y, Wang H (2015) Down-regulation of multiple CDK inhibitor ICK/KRP genes promotes cell proliferation, callus induction and plant regeneration in Arabidopsis. Front Plant Sci **6**: 1–12

Cosgrove DJ (2016) Plant cell wall extensibility: Connecting plant cell growth with cell wall structure, mechanics, and the action of wall-modifying enzymes. J Exp Bot **67**: 463–476

Cosgrove DJ (2018) Diffuse Growth of Plant Cell Walls. Plant Physiol **176**: 16–27

Coskun D, Britto DT, Shi W, Kronzucker HJ (2017) Nitrogen transformations in modern agriculture and the role of biological nitrification inhibition. Nat Plants **3**: 1–10

Crawford NM, Glass AD. (1998) Molecular and physiological aspects of nitrate uptake in plants. Trends Plant Sci **3**: 389–395

Czesnick HR, Lenhard M (2015) Size control in plants—lessons from leaves and flowers. Cold Spring Harb Perspect Biol **7**: 1–16

Dubois M, Skirycz A, Claeys H, Maleux K, Dhondt S, De Bodt S, Vanden Bossche R, De Milde L, Yoshizumi T, Matsui M, et al (2013) ETHYLENE RESPONSE FACTOR6 Acts as a Central Regulator of Leaf Growth under Water-Limiting Conditions in Arabidopsis. Plant Physiol **162**: 319–332

Duermeyer L, Khodapanahi E, Yan D, Krapp A, Rothstein SJ, Nambara E (2018) Regulation of seed dormancy and germination by nitrate. Seed Sci Res **23**: 1–8

Elsner J, Michalski M, Kwiatkowska D (2012) Spatiotemporal variation of leaf epidermal cell

growth: A quantitative analysis of Arabidopsis thaliana wild-type and triple cyclinD3 mutant plants. Ann Bot **109**: 897–910

Eng RC, Sampathkumar A (2018) Getting into shape: the mechanics behind plant morphogenesis. Curr Opin Plant Biol **46**: 25–31

Epstein E, Bloom A (2005) Mineral nutrition of plants: principles and perspectives, 2nd edn. Sunderland, MA Sinauer Assoc Inc 400

Fait A, Angelovici R, Less H, Ohad I, Urbanczyk-Wochniak E, Fernie AR, Galili G (2006) Arabidopsis Seed Development and Germination Is Associated with Temporally Distinct Metabolic Switches. Plant Physiol **142**: 839–854

Ferjani A, Horiguchi G, Yano S, Tsukaya H (2007) Analysis of Leaf Development in fugu Mutants of Arabidopsis Reveals Three Compensation Modes That Modulate Cell Expansion in Determinate Organs. Plant Physiol **144**: 988–999

Fredes I, Moreno S, Díaz FP, Gutiérrez RA (2019) Nitrate signaling and the control of Arabidopsis growth and development. Curr Opin Plant Biol **47**: 112–118

Fridlender M, Lev-Yadun S, Baburek I, Angelis K, Levy AA (1996) Cell divisions in cotyledons after germination: Localization, time course and utilization for a mutagenesis assay. Planta **199**: 307–313

Gaudinier A, Rodriguez-Medina J, Zhang L, Olson A, Liseron-Monfils C, Bågman AM, Foret J, Abbitt S, Tang M, Li B, et al (2018) Transcriptional regulation of nitrogen-associated metabolism and growth. Nature **563**: 259–264

Gegas VC, Wargent JJ, Pesquet E, Granqvist E, Paul ND, Doonan JH (2014) Endopolyploidy as a potential alternative adaptive strategy for Arabidopsis leaf size variation in response to UV-B. J Exp Bot **65**: 2757–2766

Gendreau E, Traas J, Demos T, Grandjean O, Caboche M, Hofte H (1997) Cellular Basis of Hypocotyl Crowth in Arabidopsis thaliana'. Plant Physiol **114**: 295–305

Gojon A, Krouk G, Perrine-Walker F, Laugier E (2011) Nitrate transceptor(s) in plants. J Exp Bot **62**: 2299–2308

González N, Inzé D (2015) Molecular systems governing leaf growth: From genes to networks. J Exp Bot **66**: 1045–1054

Gonzalez N, Vanhaeren H, Inzé D (2012) Leaf size control: Complex coordination of cell division and expansion. Trends Plant Sci **17**: 332–340

Gras DE, Vidal EA, Undurraga SF, Riveras E, Moreno S, Dominguez-Figueroa J, Alabadi D, Blázquez MA, Medina J, Gutiérrez RA (2018) SMZ/SNZ and gibberellin signaling are required for nitrate-elicited delay of flowering time in Arabidopsis thaliana. J Exp Bot **69**: 619–631

Green PB (1976) Growth and Cell Pattern Formation on an Axis : Critique of Concepts , Terminology , and Modes of Study. Bot Gaz **137**: 187–202

Guan P (2017) Dancing with Hormones: A Current Perspective of Nitrate Signaling and Regulation in Arabidopsis. Front Plant Sci **8**: 1–20

Guan P, Ripoll J-J, Wang R, Vuong L, Bailey-Steinitz LJ, Ye D, Crawford NM (2017) Interacting TCP and NLP transcription factors control plant responses to nitrate availability. Proc Natl Acad Sci **114**: 2419–2424

Hamdoun S, Zhang C, Gill M, Kumar N, Churchman M, Larkin JC, Kwon A, Lu H (2016) Differential Roles of Two Homologous Cyclin-Dependent Kinase Inhibitor Genes in Regulating Cell Cycle and Innate Immunity in Arabidopsis. Plant Physiol **170**: 515–527

Ho CH, Lin SH, Hu HC, Tsay YF (2009) CHL1 Functions as a Nitrate Sensor in Plants. Cell

138: 1184–1194

Hong L, Dumond M, Tsugawa S, Sapala A, Routier-Kierzkowska AL, Zhou Y, Chen C, Kiss A, Zhu M, Hamant O, et al (2016) Variable Cell Growth Yields Reproducible OrganDevelopment through Spatiotemporal Averaging. Dev Cell **38**: 15–32

Hong L, Dumond M, Zhu M, Tsugawa S, Li C-B, Boudaoud A, Hamant O, Roeder AHK (2018) Heterogeneity and Robustness in Plant Morphogenesis: From Cells to Organs. Annu Rev Plant Biol **69**: annurev-arplant-042817-040517

Horiguchi G, Tsukaya H (2011) Organ Size Regulation in Plants: Insights from Compensation. Front Plant Sci **2**: 1–6

Inzé D, De Veylder L (2006) Cell Cycle Regulation in Plant Development. Annu Rev Genet **40**: 77–105

Ishida T, Adachi S, Yoshimura M, Shimizu K, Umeda M, Sugimoto K (2010) Auxin modulates the transition from the mitotic cycle to the endocycle in Arabidopsis. Development **137**: 63–71

Jones AR, Forero-Vargas M, Withers SP, Smith RS, Traas J, Dewitte W, Murray JAH (2017) Cell-size dependent progression of the cell cycle creates homeostasis and flexibility of plant cell size. Nat Commun **8**: 1–13

Jovtchev G, Schubert V, Meister A, Barow M, Schubert I (2006) Nuclear DNA content and nuclear and cell volume are positively correlated in angiosperms. Cytogenet Genome Res **114**: 77–82

Katagiri Y, Hasegawa J, Fujikura U, Hoshino R, Matsunaga S, Tsukaya H (2016) The coordination of ploidy and cell size differs between cell layers in leaves. Development **143**: 1120–1125

Kheibarshekan Asl L, Dhondt S, Boudolf V, Beemster GTS, Beeckman T, Inze D, Govaerts W, De Veylder L (2011) Model-Based Analysis of Arabidopsis Leaf Epidermal Cells Reveals Distinct Division and Expansion Patterns for Pavement and Guard Cells. Plant Physiol **156**: 2172–2183

Kierzkowski D, Nakayama N, Routier-Kierzkowska A-L, Weber A, Bayer E, Schorderet M, Reinhardt D, Kuhlemeier C, Smith RS (2012) Elastic Domains Regulate Growth and Organogenesis in the Plant Shoot Apical Meristem. Science (80-) **335**: 1096–1099

Landrein B, Formosa-Jordan P, Malivert A, Schuster C, Melnyk CW, Yang W, Turnbull C, Meyerowitz EM, Locke JCW, Jönsson H (2018) Nitrate modulates stem cell dynamics in Arabidopsis shoot meristems through cytokinins. Proc Natl Acad Sci **115**: 1382–1387

Lee HO, Davidson JM, Duronio RJ (2010) Endoreplication : polyploidy with purpose. Genes Dev 2461–2477

Liu K, Niu Y, Konishi M, Wu Y, Du H, Sun Chung H, Li L, Boudsocq M, McCormack M, Maekawa S, et al (2017) Discovery of nitrate–CPK–NLP signalling in central nutrient–growth networks. Nature 1–23

Long Y, Boudaoud A (2019) Emergence of robust patterns from local rules during plant development. Curr Opin Plant Biol **47**: 127–137

Marchive C, Roudier F, Castaings L, Bréhaut V, Blondet E, Colot V, Meyer C, Krapp A (2013) Nuclear retention of the transcription factor NLP7 orchestrates the early response to nitrate in plants. Nat Commun **4**: 1–9

Martin T, Oswald O, Graham IA (2002) Arabidopsis Seedling Growth, Storage Lipid Mobilization, and Photosynthetic Gene Expression Are Regulated by Carbon:Nitrogen Availability. Plant Physiol **128**: 472–481

Melaragno JE (1993) Relationship between Endopolyploidy and Cell Size in Epidermal Tissue of Arabidopsis. Plant Cell Online **5**: 1661–1668

Merigout P, Lelandais M, Bitton F, Renou J-P, Briand X, Meyer C, Daniel-Vedele F (2008) Physiological and Transcriptomic Aspects of Urea Uptake and Assimilation in Arabidopsis Plants. Plant Physiol **147**: 1225–1238

Noir S, Bomer M, Takahashi N, Ishida T, Tsui T-L, Balbi V, Shanahan H, Sugimoto K, Devoto A (2013) Jasmonate Controls Leaf Growth by Repressing Cell Proliferation and the Onset of Endoreduplication while Maintaining a Potential Stand-By Mode. Plant Physiol **161**: 1930–1951

O'Malley RC, Huang SSC, Song L, Lewsey MG, Bartlett A, Nery JR, Galli M, Gallavotti A, Ecker JR (2016) Cistrome and Epicistrome Features Shape the Regulatory DNA Landscape. Cell **165**: 1280–1292

Poitout A, Crabos A, Petřík I, Novák O, Krouk G, Lacombe B, Ruffel S (2018) Responses to Systemic Nitrogen Signaling in Arabidopsis Roots Involve *trans* -Zeatin in Shoots. Plant Cell **30**: 1243–1257

Powell AE, Lenhard M (2012) Control of organ size in plants. Curr Biol **22**: R360–R367

Rahayu YS, Walch-Liu P, Neumann G, Römheld V, Von Wirén N, Bangerth F (2005) Root-derived cytokinins as long-distance signals for NO3--induced stimulation of leaf growth. J Exp Bot **56**: 1143–1152

Riveras E, Alvarez JM, Vidal EA, Oses C, Vega A, Gutiérrez RA (2015) The Calcium Ion Is a Second Messenger in the Nitrate Signaling Pathway of Arabidopsis. Plant Physiol **169**: 1397–1404

Robinson DO, Coate JE, Singh A, Hong L, Bush M, Jeff J (2018) Ploidy and Size at Multiple

Scales in the Arabidopsis Sepal. Plant Cell. doi: 10.1105/tpc.18.00344

Roeder AHK, Chickarmane V, Cunha A, Obara B, Manjunath BS, Meyerowitz EM (2010) Variability in the control of cell division underlies sepal epidermal patterning in Arabidopsis thaliana. PLoS Biol. doi: 10.1371/journal.pbio.1000367

Roeder AHK, Cunha A, Ohno CK, Meyerowitz EM (2012) Cell cycle regulates cell type in the Arabidopsis sepal. Dev **139**: 4416–4427

Savaldi-Goldstein S, Peto C, Chory J (2007) The epidermis both drives and restricts plant shoot growth. Nature **446**: 199–202

Scholes DR, Paige KN (2015) Plasticity in ploidy: A generalized response to stress. Trends Plant Sci **20**: 165–175

Serrano-Mislata A, Schiessl K, Sablowski R (2015) Active Control of Cell Size Generates Spatial Detail during Plant Organogenesis. Curr Biol **25**: 2991–2996

Sliwinska E, Bassel GW, Bewley JD (2009) Germination of Arabidopsis thaliana seeds is not completed as a result of elongation of the radicle but of the adjacent transition zone and lower hypocotyl. J Exp Bot **60**: 3587–3594

Stoynova-Bakalova E, Karanov E, Petrov P, Hall MA (2004) Cell division and cell expansion in cotyledons of Arabidopsis seedlings. New Phytol **162**: 471–479

Sun C-H, Yu J-Q, Hu D-G (2017) Nitrate: A Crucial Signal during Lateral Roots Development. Front Plant Sci. doi: 10.3389/fpls.2017.00485

Takahashi N, Kajihara T, Okamura C, Kim Y, Katagiri Y, Okushima Y, Matsunaga S, Hwang I, Umeda M (2013) Cytokinins control endocycle onset by promoting the expression of an APC/C activator in arabidopsis roots. Curr Biol **23**: 1812–1817

Takei K, Sakakibara H, Taniguchi M, Sugiyama T (2001) Nitrogen-dependent accumulation

of cytokinins in root and the translocation to leaf: Implication of cytokinin species that induces gene expression of maize response regulator. Plant Cell Physiol **42**: 85–93

Takei K, Ueda N, Aoki K, Kuromori T, Hirayama T, Shinozaki K, Yamaya T, Sakakibara H (2004) AtIPT3 is a key determinant of nitrate-dependent cytokinin biosynthesis in Arabidopsis. Plant Cell Physiol **45**: 1053–1062

Tauriello G, Meyer HM, Smith RS, Koumoutsakos P, Roeder AHK (2015) Variability and constancy in cellular growth of Arabidopsis sepals. Plant Physiol **169**: pp.00839.2015

Tian T, Liu Y, Yan H, You Q, Yi X, Du Z, Xu W, Su Z (2017) AgriGO v2.0: A GO analysis toolkit for the agricultural community, 2017 update. Nucleic Acids Res **45**: W122–W129

Tsukaya H (2019) Has the impact of endoreduplication on cell size been overestimated? New Phytol **223**: 11–15

Tsukaya H, Tsuge T, Uchimiya H (1994) The cotyledon: A superior system for studies of leaf development. Planta **195**: 309–312

Uyttewaal M, Burian A, Alim K, Landrein B, Borowska-Wykrt D, Dedieu A, Peaucelle A, Ludynia M, Traas J, Boudaoud A, et al (2012) Mechanical stress acts via Katanin to amplify differences in growth rate between adjacent cells in Arabidopsis. Cell **149**: 439–451

Varala K, Marshall-Colón A, Cirrone J, Brooks MD, Pasquino A V, Léran S, Mittal S, Rock TM, Edwards MB, Kim GJ, et al (2018) Temporal transcriptional logic of dynamic regulatory networks underlying nitrogen signaling and use in plants. Proc Natl Acad Sciences

de Veylder L, Larkin JC, Schnittger A (2011) Molecular control and function of endoreplication in development and physiology. Trends Plant Sci **16**: 624–634

Yuan S, Zhang Z-W, Zheng C, Zhao Z-Y, Wang Y, Feng L-Y, Niu G, Wang C-Q, Wang J-

H, Feng H, et al (2016) *Arabidopsis* cryptochrome 1 functions in nitrogen regulation of flowering. Proc Natl Acad Sci **113**: 7661–7666